The Geological Society Special Publications

Insights into the Early Evolution of the Côte d'Ivoire Margin (West Africa)

--Manuscript Draft--

Manuscript Number:	GSLSpecPub17-086R4
Article Type:	Chapter
Full Title:	Insights into the Early Evolution of the Côte d'Ivoire Margin (West Africa)
Short Title:	Early Evolution of the Côte d'Ivoire Margin
Corresponding Author:	Nicola Scarselli Royal Holloway University of London UNITED KINGDOM
Corresponding Author E-Mail:	n.scarselli@es.rhul.ac.uk
Other Authors:	Gregor Duval
	Javier Martin
	Ken McClay
	Steve Toothill
Order of Authors (with Contributor Roles):	Nicola Scarselli (Investigation: Lead; Visualization: Lead; Writing – original draft: Lead; Writing – review & editing: Equal)
	Gregor Duval (Writing – original draft: Supporting; Writing – review & editing: Equal)
	Javier Martin (Writing – review & editing: Equal)
	Ken McClay (Writing – review & editing: Supporting)
	Steve Toothill (Writing – review & editing: Equal)
Abstract:	A tectono-stratigraphic analysis of a broadband 3D seismic survey over the outer slope of Côte d'Ivoire margin, west Africa, revealed that Cenomanian and younger strata seal well-developed rift fault blocks up to 15 km across. Growth strata indicate that these were formed during rifting that culminated in seafloor spreading in the late Albian, challenging existing plate reconstructions for the opening of the equatorial Atlantic ocean. A previously unrecognised system of volcanic edifices linked at depth to an network of sill complexes has also been identified. These are aligned along a NE-SW trend, concordant with km-wide ridges, interpreted as folds formed by steep, crustal faults with an oblique-slip component. These trends are similar to those of fracture zones in the region and indicate that the Côte d'Ivoire was a transform margin in the Late Albian. These results highlight the potential of offshore Côte d'Ivoire for deepwater rift plays with large traps formed by extensional fault blocks together with prospective Albian turbidite reservoirs ponded in their hangingwalls. In addition, the volcanoes and ridges generated seabed relief along the newly-created transform margin, forming confined basins for potential deposition of Turonian and younger turbidites and the generation of stratigraphic traps.
Section/Category:	Passive Margins: Tectonics, Sedimentation and Magmatism
Additional Information:	
Question	**Response**
Are there any conflicting interests, financial or otherwise?	No
Samples used for data or illustrations in this article have been collected in a responsible manner	Confirmed

Insights into the Early Evolution of the Côte d'Ivoire Margin (West Africa)

Nicola Scarselli[1*], Gregor Duval[2], Javier Martin[2], Ken McClay[1], Steve Toothill[2]

1. Department of Earth Sciences, Royal Holloway University of London, Egham, TW20 0EX, Surrey, United Kingdom

2. CGG, Crompton Way, Crawley, RH10 9QN, West Sussex, United Kingdom

* Corresponding author (e-mail: nicola.scarselli@rhul.ac.uk)

Abbreviated title: Early Evolution of the Côte d'Ivoire Margin

Abstract

A tectono-stratigraphic analysis of a broadband 3D seismic survey over the outer slope of Côte d'Ivoire margin, west Africa, revealed that Cenomanian and younger strata seal well-developed rift fault blocks up to 15 km across. Growth strata indicate that these were formed during rifting that culminated in seafloor spreading in the late Albian, challenging existing plate reconstructions for the opening of the equatorial Atlantic ocean. A previously unrecognised system of volcanic edifices linked at depth to a network of sill complexes has also been identified. These are aligned along a NE–SW trend, concordant with kilometre-wide ridges, interpreted as folds formed by steep, crustal faults with an oblique-slip component. These trends are similar to those of fracture zones in the region and indicate that the Côte d'Ivoire was a transform margin in the late Albian.

These results highlight the potential of offshore Côte d'Ivoire for deepwater rift plays with large traps formed by extensional fault blocks together with prospective Albian turbidite reservoirs ponded in their hangingwalls. In addition, the volcanoes and ridges generated seabed relief along the newly-created transform margin, forming confined basins for potential deposition of Turonian and younger turbidites and the generation of stratigraphic traps.

Keywords: Côte d'Ivoire, West Africa, deep-water, hydrocarbons

Recent exploration success in the mid-slope offshore Ghana and Côte d'Ivoire (Fig. 1; Dailly et al., 2013; Martin et al., 2015) has prompted interest in the tectono-stratigraphic evolution and hydrocarbon potential of the equatorial African margin (Dailly et al., 2013; Coole et al., 2015; Davison et al., 2015; Martin et al., 2015; Nemčok et al., 2013, 2016; Sabato Ceraldi et al., 2016; Ye et al., 2017). The basins along this margin, especially those located offshore Côte d'Ivoire and Ghana, and in particular their deep-water sectors, are regarded as being poorly understood due to limited drilling beyond the shelf break (Wells et al., 2012). Previous research was based on analyses of a coarse grid of 2D seismic lines mainly acquired across the Côte d'Ivoire-Ghana ridge, leaving the adjacent basins largely unexplored (Mascle & Blarez, 1987; Basile et al., 1993; Sage et al., 2000; Attoh et al., 2004; Antobreh et al., 2009;). Since the work of Antobreh *et al.* (2009) no research based on the analysis of new geophysical data acquired in the deep-water of Côte d'Ivoire has been published.

A number of plate tectonic models for the opening of the South Atlantic ocean, including the equatorial African margin, have been proposed over the last 25 years (e.g. Nürnberg & Müller, 1991; Jones et al., 1995; Eagles, 2007; Moulin et al., 2010; Heine et al., 2013; Granot & Dyment, 2015; Pérez-Díaz & Eagles, 2014). These models are mainly driven by ages of seafloor spreading based on the recognition of magnetic anomalies. As a result different models have been proposed for the equatorial African margin due to the lack of magnetic anomalies in the Equator–magnetic 'quiet zone' (Rabinowitz & LaBrecque, 1979; Clift et al., 1997; Antobreh et al., 2009; Granot & Dyment, 2015), adding to uncertainties related to the timing of rifting and seafloor spreading along the margin.

This paper presents the interpretation of a high-quality, depth-migrated, 3D broadband seismic survey over a large, virtually unexplored area, in the deep-water Ivorian Tano basin offshore Côte d'Ivoire (Fig. 1; Martin et al. 2015). Broadband technology has allowed deep penetration and provides high-quality images of features at depths in excess of 10 km below sea-level. The research provides an understanding of the early geological history offshore Côte d'Ivoire margin, with new evidence that constrains previously unrecognised tectonic phases. The wider implications of this research on the evolution of nearby basins along the equatorial African margin are also discussed.

Geological Setting

The Côte d'Ivoire and Ghana shelf is regarded as a world-class example of a transform margin (Attoh et al., 2004; Antobreh et al., 2009; Nemčok et al., 2013; Basile, 2015; Mercier de Lépinay et al., 2016). Seminal papers on transform margins were based on the analysis of the Côte d'Ivoire–Ghana ridge (e.g. Mascle & Blarez, 1987), a prominent bathymetric feature that is thought to be related to the activation of the Romanche fracture zone, the largest transform fault and fracture system known with maximum lateral offset of the Mid-Atlantic ridge of ~800 km (e.g. Davison et al., 2015).

The shallow water of the Côte d'Ivoire margin is relatively well explored with a number of wells drilled and several seismic acquisition campaigns since the '70s (Attoh et al., 2004; Brownfield & Charpentier, 2006; Antobreh et al., 2009; Martin et al., 2015). These investigations indicated the presence of Cretaceous strata in a series of rift depocentres commonly referred to as the Ivorian Coastal Basin (Figs. 1, 2 & 3; Attoh et al. 2004; Antobreh et al. 2009). Within these basins, terrestrial to shallow marine sediments of Aptian–Albian age have been drilled and found to contain reservoirs and source rocks of good quality (Fig. 2; Dailly et al., 2013; Martin et al., 2015). These units are offset by extensional faults that are sealed by Upper Cretaceous and younger sediments, and therefore the Aptian–Albian section has been regarded as a syn-rift sequence (Mascle & Blarez, 1987; Basile et al., 1993; Antobreh et al., 2009). However, the previous research did not investigate the geometries of growth strata around these faults in order to elucidate timing of rifting and 'break-up'.

The timing of seafloor spreading and onset of post-rift conditions along the Côte d'Ivoire margin is contentious. The age proposed by plate tectonic models varies from late Aptian (Heine et al., 2013) to mid-Albian (Antobreh et al., 2009; Torsvik et al., 2009; Mercier de Lépinay et al., 2016) to late Albian (Eagles, 2007; Pérez-Díaz & Eagles, 2014). Well penetrations in the shelf sector of the margin sampled post-rift Cenomanian marine siliciclastics and carbonates sealing fault-block crests (Fig. 2; Dumestre, 1985; Chierici, 1996; Brownfield & Charpentier, 2006). Within this Upper Cretaceous post-rift section, a successful mid-slope play was proven by the Mahogany-1 discovery in Ghana (Jubilee field) and followed up recently in the Côte d'Ivoire with Anadarko's Paon, Pelican and Rossignol discoveries (Figs. 1, 2 & 3; Dailly et al., 2013; Martin et al., 2015).

In the sequence of events from rift to drift, it is thought that shear stresses due to progressive development of the transform margin may have played a major role in the development of the Ivorian Tano basin (Mascle & Blarez, 1987; Antobreh et al., 2009). However, geological evidence is scant, primarily due to the uncertainties related to the interpretation of structures using widely spaced 2D lines.

Seismic data

The dataset available for this study was a 3000 km^2 subset of a larger 3D seismic volume which covers 4400 km^2 of the Côte d'Ivoire outer slope. The volume is located ~ 25 km south of the recent Paon discovery, at a Present-Day water depth of 2 km (Figs. 1 & 3).

The dataset was acquired in 2014 by CGG using the latest broadband technology which allows enhanced low-frequency content for a deeper penetration, and in turn provides for clearer imaging at depth (Firth et al., 2014; Hill et al., 2006). The dataset was processed with 3D Kirchhoff PSDM (Pre-Stack Depth Migration) to a depth of 12 km. Processing included advanced de-multiple and de-ghosting techniques such as 3D SRME (Surface Related Multiple Elimination) and GWE (Ghost Wavefield Elimination) to obtain the sharpest images possible. The velocity model used to drive the PSDM was obtained from ray-based tomography. The main velocity boundaries were built using a classic layer-stripping top-to-bottom approach encompassing a total of 12 iterations and making use of the following structural markers: water bottom, Eocene, Campanian, Turonian and Albian boundaries. Anisotropy was accounted for through a TTI approach (Tilted Transverse Isotropy) in which the velocity parameters parallel to the structural horizon planes are isotropic but may differ perpendicularly to the structural trends. This research, which focuses on deep structures at depth of 5–12 km (e.g. Fig. 4), has greatly benefited from this advanced seismic acquisition and processing techniques.

The dataset is zero-phased and processed following the Society of Exploration Geophysicists (SEG) amplitude polarity convention. 'Hard kicks' (an increase in acoustic impedance with depth) correspond to a positive reflection that appears grey to black in the seismic displays shown in this paper. Conversely, 'soft kicks' correspond to red-yellow reflections.

There was no well data directly available within the area covered by the survey. Seismic stratigraphy was calibrated by correlation of picks from wells outside the survey area, along regional 2D seismic lines intersecting the 3D survey. The correlation of Top Albian, Top Cenomanian and Top Turonian is considered to be good as these horizons were not affected by major unconformities or large faults (Fig. 4). The correlation of the Mid Albian horizon has a degree of uncertainty as this is offset by prominent faults. However, this stratigraphic pick was tied to a high amplitude continuous reflection which is easily identifiable in the data (Fig. 4).

Interpretation workflow

Seismic analysis was carried out using Halliburton Geoprobe and DecisionSpace Desktop tools using established 3D seismic interpretation techniques (e.g. Cartwright & Huuse, 2005; Posamentier et al., 2007). Standard workflows have been enhanced through the utilisation of seismic attributes such as dip-steered coherency and reflection strength. Coherency was used to highlight faults (Bahorich & Farmer, 1995; Marfurt et al., 1998; Chopra & Marfurt, 2008; Iacopini & Butler, 2011;). The dip-steering variant of the attribute was implemented so to achieve improved fault detection (de Groot & Bril, 2005; Marfurt & Alves, 2015). Reflection strength, also known as envelope or instantaneous amplitude (Barnes, 2007; Chopra & Marfurt, 2007) was used to accentuate amplitude variations and to highlight high-amplitude features such as igneous intrusions.

Key seismic horizons and depth-slices have been interpreted to gather an understanding of the geology of the area of interest (Figs. 4 & 5). Interpretation of the Mid Albian horizon was key in revealing a well-developed fault system at depth (Fig. 6). The Top Albian was also an important horizon as its interpretation showed a series of prominent ridges and younger faults (e.g. Figs. 9 & 10). Where observed, growth strata geometries were studied to constrain timing of fault activation (McClay, 1990; McClay and Ellis, 1987). The Top Cenomanian and a depth-slice at 7.5 km were also interpreted to map the magmatic system of volcanoes and sills (Fig. 12).

Seismic Stratigraphy

Figure 4 is a seismic stratigraphic diagram that focuses on the lower half of the survey where deep structures and Lower to Upper Cretaceous strata are clearly imaged. At the base of the survey (depth ~11 km), the top of seismic basement horizon divides a low amplitude, chaotic to reflection-free unit from a package with well-developed reflectivity above. This vertical arrangement of seismic facies suggests a transition from the seismic basement to a sedimentary cover above.

The age of the strata at the base of the sedimentary pile cannot be constrained. However, given that there are over 3 km of sediments below the Mid Albian horizon, it is proposed that the sediments immediately above the basement are lower Albian, possibly Aptian in age. These strata, together with the upper Albian, form a section up to 4 km thick, seismically characterised by prominent reflections with variable amplitudes. This package is offset by large normal faults which appear to terminate at depths of 11 to 12 km, possibly indicating the presence of a low-angle detachment (Figs. 4, 5, 7 & 8). The Aptian to Albian units exhibit evidence of incisions several kilometres across (Figs. 7 & 8) and, in places, are characterised by the presence of high amplitude events, interpreted to be sills and dykes (Figs. 4 & 5). These intrusions are elements of a large magmatic system imaged in the western-central part of the survey (see following sections and Figure 12).

The Top Albian is a prominent, high amplitude, continuous reflection that can be easily traced over a large extent of the 3D seismic volume as well as in nearby 2D seismic lines. The mapped horizon divides deformed Albian strata from packages of flat, mainly undeformed, continuous reflections of the Cenomanian, Turonian and Coniacian units (Fig. 4). The Top Cenomanian and Top Turonian seismic picks provide further subdivision within the upper Lower Cretaceous and Upper Cretaceous strata imaged within the survey.

Fault styles and timings

1st generation faults

The depth structure map of the Mid Albian horizon documents the presence of a well-developed, NW–SE trending (mean strike 319º, n=8), extensional fault system (Fig. 6). The presence of a large intrusive system meant that reliable interpretation of the Mid Albian horizon was possible only in restricted areas of the eastern part of the seismic survey (Figs. 5 & 6). Here, individual faults were observed to extend laterally for 4–6 km, with large faults continuing well beyond the survey boundaries, possibly reaching lengths in excess of 10–20 km (Fig. 6).

Dip-oriented profiles in Figures 7 & 8 show that the fault system developed a variety of extensional geometries including half-grabens, horst and grabens as well as domino fault blocks. Individual fault blocks are commonly 3–15 km across and exhibit pronounced rotation, reaching values in excess of 35º along the larger faults. The block-bounding faults are planar and are characterised by shallow fault dips of 20º–35º. Where seismic imaging allows clear mapping of the faults at depth, it can be seen that these progressively become listric as they sole onto the deep detachment level (Figs. 7 & 8). Large faults extend vertically for up to 2.5 km and can attain maximum displacements in excess of 1.5 km at the mid-Albian level (Fig. 7).

The hanging walls of the faults have fanning growth strata with geometries that thicken against the faults indicating progressive rotation as extension developed (Fig. 8). In places these growth strata can exceed thicknesses of 3.5 km within the Aptian to Albian succession suggesting a long-lived phase of extension at that time. Investigation of stratal terminations reveals truncations below the Mid Albian horizon (Figs. 7 & 8) which could possibly indicate two phases of extension on these faults.

2nd generation faults

Detailed analysis of the depth structure map and coherency extractions along the Top Albian horizon reveals numerous extensional faults affecting the uppermost part of the Albian strata (Figs. 9, 10a & 11). The faults are abundant in the eastern part of the survey (Figs. 9a & c) and have an overall NW–SE trend (mean strike trend 328º; n=42; Fig. 9). Attribute extractions and 3D views show that these faults are straight or slightly curvilinear with fault lengths of 1.5 to 8 km (Figs. 9b & 10a).

Vertical profiles perpendicular to the faults show that these are planar with fault dips of ~ 50º (Fig. 11). Large faults can attain offsets of ~150 m and extend vertically for ~ 2 km, offsetting the upper Albian and lower Cenomanian strata. In places, these structures seem to be linked to the larger '1st generation' faults at depth (Fig. 8).

Given the limited displacement of these faults, growth strata are not readily apparent, limiting the determination of their exact age. However, the faults are sealed by the Top Cenomanian horizon but offset the Top Albian horizon (Fig. 11). Therefore, these relationships possibly indicate fault activity during the Cenomanian.

Ridges

Depth structure maps of the Mid Albian horizon (Fig. 6) and Top Albian horizon (Figs. 9 & 10a) show a series of prominent, NE–SW-trending ridges (mean strike trend 49º, n=26; Fig. 9c). The ridges range in length from 1.5 to 5 km with widths ranging from 500 m to 2 km (Figs. 9 & 10a). Large ridges with widths in excess of 5 km seem to be formed by a number of coalesced structures (Fig. 10a). Three-dimensional displays of the Top Albian horizon show clear examples of ridges arranged in 'en echelon' fashion as well as examples of the Cenomanian faults offsetting, hence postdating, the ridges. Vertical profiles through the ridges reveal these features pertain to upper Albian and Cenomanian strata and are asymmetric, with steep limbs of 25º–30º and shallow limbs of 15º–20º (Fig. 10b). It is noted that asymmetry of the limbs changes along the same trend of ridges (Fig. 10a).

The 'en echelon' array of the ridges and their marked asymmetry may indicate that these features are fault-propagation folds controlled by steep faults at depth with a component of oblique slip. Lateral variations in their asymmetry also suggests an along strike variation in direction of dip of the faults at depth (Fig. 10b). The marked asymmetry of the ridges makes an alternative explanation of a volcanic origin less preferable. Thickness variations across the ridges as well as onlap terminations toward their crests can be clearly observed within the section bounded by Top Cenomanian and the Mid Albian horizons. These indicate a long-lived phase of growth of the ridges during the late Albian and Cenomanian.

Magmatic system

Volcanoes

Three prominent, sub-circular to elliptical mounds are shown in the depth-structure maps of the Top Albian and Top Cenomanian (Figs. 9 & 12a). The mounds are aligned in a NE–SW direction, which is similar to the strike trend of the ridges described above (Fig. 9). The mounds are spatially related to high amplitude features at depth that are interpreted to be igneous sills forming an extensive magmatic system observed in the eastern part of the survey (Fig. 12a). For this reason, the mounds are ascribed to be the effusive part of such magmatic system.

Detailed interpretation of vertical profiles shows a clear volcanic stratigraphy embedded between two key surfaces, the top and the base of volcanoes (Fig. 13). The top volcano is a composite surface defined by a series of clear onlap terminations of Lower Cretaceous strata onto the volcanic edifices. The oldest onlapping strata are the uppermost Albian, capped by the Top Albian horizon that also terminates against the flanks of the volcanoes. These features suggests that extrusion and therefore formation of the magmatic system ended in the late Albian.

Below the top volcano surface, a series of well-imaged reflections dip away from the volcanic crest. These units, which are inferred to be mid-Albian in age, mimic the shape of the flanks of the volcano and are therefore interpreted to be a series of volcanoclastic deposits forming the main body of the volcanic structure (Figs. 12 & 13). These strata terminate downwards in a series of well-imaged downlaps that define the base of the volcano - i.e. the paleo-depositional surface at the time of extrusion (Fig. 13). It is noted that the base volcano horizon is stratigraphically located well above the Mid Albian horizon, suggesting that volcanic extrusion likely initiated in the mid to late Albian. Interpretation of the top and base volcano horizons shows that the volcanoes have basal widths from 7 to 10 km, with current heights in excess of 1.5 km and flank dips of ~25º. These large geomorphic features undoubtedly had significant impact on the stratal architectures of the Upper Cretaceous stratigraphy as demonstrated by onlap terminations of Cenomanian and Turonian units as well as drape structures in Coniacian and younger strata.

Sills

Reflection strength extractions at a depth of 7.5 km reveals a subcircular area with a diameter of ~70 km characterised by high amplitude responses in the western part of the dataset (Fig. 12b). Detailed inspection shows numerous high amplitude bodies 2 to 8 km wide (Figs. 12b & c). On vertical seismic sections these have hard reflections that are parallel to the stratigraphy (e.g. Figs. 7, 12 & 13), the typical diagnostic characteristics of igneous sills (e.g. Hansen et al., 2004). The sill complexes extend over an area of 2900 km^2 centred around the volcanic edifices (Figs. 12a & b). For this reason, it is interpreted that volcanoes and sills are part of the same magma system (Fig. 12). The lack of definitive age-diagnostic features, such as onlap terminations against sill-inflation anticlines, means that the timing of emplacement of the sill complexes is not constrained. However, it is assumed that sills are genetically related to the volcanics, forming the intrusive counterpart of the same magmatic system. This implies that the sills may have been emplaced slightly earlier or at the same time as the volcanoes formed, during the mid to late Albian.

Discussion

Rift-drift evolution of the Côte d'Ivoire margin

The results of this research show clear evidence of long-lived extension on the Côte d'Ivoire margin along NW–SE-trending faults that started in the Aptian and ended in the late Albian (Fig. 14). The resultant structures, with shallow, somewhat listric faults detached onto a low-angle detachment with highly-rotated fault blocks (Figs. 7 & 8). The detachment is probably located within the basement unit, and this together with the orientations of the faults along expected regional rift trends, suggests that the extensional faults in this survey are related to the rift processes as the South Atlantic opened in the Early Cretaceous.

Hyper-extended rifted basins commonly display faults that detach above weak exhumed, serpentinised mantle (Doré & Lundin, 2015). Seismic profiles from the west Iberia margin have shown low-angle, listric faults with fault dips of 20º–30º that define fault blocks with rotations of 10º to 30º (Reston and Pérez-Gussinyé, 2007; Ranero & Pérez-Gussinyé, 2010; Bayrakci et al., 2016). A similar hyper-extension model may be invoked to explain the structural styles of the extensional faults observed offshore Côte d'Ivoire (Fig. 3). This may also be supported by analyses of refraction surveys and potential field data that indicate the presence of anomalously thin oceanic crust and serpentinised lower crustal bodies near the continent-ocean boundary on the margin (Peirce et al., 1996; Antobreh et al., 2009).

Margin break-up

The timing of break-up from this study is constrained by the Top Albian horizon that clearly seals underlying syn-rift growth strata (Figs. 6 & 7). This would imply seafloor spreading and a full marine environment offshore Côte d'Ivoire since Cenomanian time (100.5 Ma; Fig. 14a). This timing of break-up challenges some well-established plate reconstruction of the South Atlantic (Antobreh et al., 2009; Torsvik et al., 2009; Heine et al., 2013; Mercier de Lépinay et al., 2016) that indicate seafloor spreading in this segment of the Equatorial African Margin during Aptian–mid-Albian. Other models from Pérez-Díaz & Eagles (2014), Granot & Dyment (2015) and Eagles (2007) predict a later break-up in the late Albian–Cenomanian, more in line with the findings of this research. Analysis of sedimentary facies (Pletsch et al., 2001) and stable isotope analyses from exceptionally well-preserved foraminifera from a number of ODP sites along the equatorial African margin (Friedrich et al., 2012) also support a late break-up as indicated by evidence that fully developed Atlantic circulation did not occur earlier than the mid Cenomanian (Granot and Dyment, 2015).

Extension along the margin was complex as shown by two distinct phases of stretching separated by an unconformity of mid-Albian age, and the partially coeval development of ridges and volcanism (Fig. 14a). The first phase of rifting in the Aptian? to early Albian corresponds to the time continental stretching initiated the formation of the Ivorian Tano Basin (Fig. 15a). It is envisaged that the mid-Albian unconformity likely represents a time of thermally-driven uplift and erosion in response to the development of a hot spreading centre to the south of the basin as stretching in the Ghana sector (to the east) of the Equatorial African Margin culminated into seafloor spreading and formation of a mid-oceanic ridge (Figs. 14a & 15b). As the unconformity is embedded within the syn-rift growth sequence (Figs. 4, 6 & 7), it implies that the mid-Albian phase of uplift erosion happened when rift conditions persisted in the Ivorian Tano basin (Fig. 15b). The occurrence of this basin-wide event is also supported by studies on thermal diagenesis of clay minerals carried out on samples recovered from ODP sites along the Côte d'Ivoire-Ghana ridge, that have identified the onset in the mid–late Albian of an abnormal and short-lived paleo-geothermal gradient of ~350°C/km (Holmes, 1998). Similarly, Holmes

(1998) and Antobreh et al. (2009) have indicated that this thermal event may have been induced by the passage of a seafloor-spreading centre south of the Ivorian Tano basin which promoted and amplified the uplift of the Côte d'Ivoire-Ghana ridge. The accretion of new oceanic crust to the south of the Ivorian Tano basin would imply the birth of an active transform margin and of the Romanche fracture zone in the mid-Albian (Fig. 15b).

Magmatism

High rates of melt supply at the base of mid-oceanic ridges are thought to be responsible for formation of steady state magma chambers along the length of ridge axes (Kelley et al., 2002; Sinton & Detrick, 1992). Here it is proposed that the magmatic system found in the Ivorian Tano basin (Figs. 11 & 12) was linked to the magmatism associated with the mid-oceanic ridge that was supposedly located at the southern end of the basin during the mid to late Albian (Fig. 15b). This is supported by the fact that magmatism ceased in the Cenomanian (Fig. 14a), a time when, once rifting had ceased, seafloor spreading and accretion of oceanic crust progressively moved the Ivorian Tano basin to the east, away from the mid-oceanic ridge to the south (Fig. 15c). Rift-related magmatism as an alternative interpretation for the genesis of the Ivorian magmatic system seems less plausible as volcanic activity was short-lived and only occurred at the latest stage of rifting (Fig. 14a).

Transform margin

The onset of a fully developed transform margin was also accompanied by the formation of the numerous mid-Albian–Cenomanian ridges observed in the study area (Figs. 9 & 10). With a strike trend similar to that of the Romanche fracture zone

(Fig. 14b), the lack of laterally consistent vergence of these structures together with their observed 'en echelon' arrangement (Fig. 10), suggest that the ridges may have developed as result of oblique slip along crustal faults that accommodated shear stresses that ensued from the development of the transform margin. Evidence of folding as the mechanism of formation of the ridges may suggest that these crustal fractures are likely to be laterally complex with stepovers and bends. Such complexities are known to partition strands of strike-slip faults with distinct styles including folds and 'narrow push-up ridges' parallel to associated fault segments (Christie-Blick & Biddle, 1985; Cunningham et al., 2007). Other ridges of similar age have been reported to exist along the equatorial African margin and have been ascribed to be inversion anticlines (Tari 2006, Antobreh et al., 2009; Davison et al., 2015). In this study, however, no 'harpoon' structures (*sensu* Badley et al. 1989) were observed to occur associated with the ridges, and these are clearly oriented perpendicularly to the extensional fault systems (Fig. 6). This makes tectonic inversion a less preferable mechanism for the formation of the ridges in the Ivorian Tano basin.

The fact that the volcanoes are aligned in the same direction as the strike trends of the ridges suggests that these deep structures may have developed as 'weak zones' allowing magma passage to the surface. The fact that the ridges became inactive in the late Cenomanian indicate the end of tectonic shearing in the Ivorian Tano basin at that time. It is proposed that this coincided with when the basin finally slid past the southern spreading centre and entered the so-called 'passive transform margin stage' (Fig. 15c; *sensu* Mascle & Blarez, 1987; Basile, 2015; Mercier de Lépinay et al., 2016).

Cenomanian extensional faults

The last structural event documented in the basin is marked by the formation of short-lived, normal faults during the Cenomanian (Figs. 11 & 14). Given their small size and limited displacements, these have not been described in previous papers that relied mainly on the analysis of widely-spaced 2D seismic lines (Attoh et al., 2004; Antobreh et al., 2009).

The Cenomanian faults have a similar orientation to the rift faults to which they seem to be linked at depth (Fig. 14b). This suggests that the Cenomanian faults formed as a result of a phase of reactivation of the older and deeper rift structures. Given the evidence that rifting terminated in the late Albian (Fig. 14b), the extensional phase responsible for the formation of these late faults may have been triggered by processes of 'post-rift relaxation' (Morgan, 1983; Burov & Cloetingh, 1997; Burov & Poliakov, 2003;). The lack of known regional tectonic events in the margin during the Late Cretaceous makes it difficult to suggest alternative scenarios for the formation of the Cenomanian faults.

Implications for hydrocarbon prospectivity

The presence of a well-developed rift architecture (Figs. 7 & 8) in the deep water Ivorian Tano basin provides additional opportunities for structural trapping in a basin thus far mostly reliant on subtle, post-rift, stratigraphic traps (Dailly et al., 2013; MacGregor et al., 2003). Within such a deep-water rift play, key controls on reservoir distribution would be in hanging wall basins where shallow marine and terrestrial drainage is likely to develop as indicated by incisions in the hangingwall of rift structures mapped in the study area (Figs. 2, 3, 7 & 8). Mid to upper Albian reservoirs have been found to be of good quality in well penetrations on the shelf of the Côte d'Ivoire margin (MacGregor et al., 2003). Lowermost Cretaceous, lacustrine, rift source rocks documented in the western Niger Delta (Haack et al., 2000) are thought to be present in similar basins along the equatorial African margin, including in the Ivorian Tano basin (Elvsborg and Dalode, 1985; MacGregor et al., 2003; Brownfield & Charpentier, 2006). Proven rift source rocks offshore Côte d'Ivoire are found in the mid and upper Albian (Morrison et al., 2000; MacGregor et al., 2003). Therefore, contingent upon a favourable timing of migration and charge, the thick rift section documented in this study is likely to contain some of these source rocks able to charge rift reservoirs in large, fault controlled traps (Fig. 3). An additional trapping mechanism in the rift play may come from the ridges (Figs. 9 & 10). These can be up to 5 km long, 1.5 km wide with over 100 m of vertical relief and hence may offer considerable trap potential. The trapping potential is much higher for coalesced ridges that may be five times longer than individual ridges (Fig. 10a). As the Cenomanian post-rift faults have offset part of the upper Albian rift section (Fig. 11), they may pose a risk for seal integrity for shallower rift reservoirs. Migration along these faults, however, would have the potential to allow charging of deep-water post-rift reservoirs from rift source rocks. Additional post-rift charge may come from well-known Cenomanian source rocks on the equatorial African margin (Morrison et al., 2000; MacGregor et al., 2003; Dailly et al., 2013). Recent exploration effort has documented the presence of high quality Upper Cretaceous turbidite reservoirs in the inner slope offshore Ghana (Jubilee field) and Côte d'Ivoire (Paon discovery) (Fig. 1; Dailly et al. 2013; Coole et al. 2015; Martin et al. 2015). Detailed seismic analysis and drilling have indicated that these reservoirs extend into the deep-water of the Ivorian Tano basin (Martin et al., 2015). Here the main control on distribution of these sands would be the post-rift seabed geomorphology, that this research has demonstrated to likely be affected by the presence of prominent volcanoes and ridges (Figs. 10, 12 & 13). These features, which may be ultimately related to deep crustal transforms, could develop confined basins where turbidite flows of Turonian to Campanian age would possibly pond, whereas highs would form barriers against which sands would onlap and pinch-out, creating potential for accumulation of reservoirs and opportunity for stratigraphic traps to develop. The recent discoveries of Pelican and Rossignol (Fig. 1b) confirm that such an Upper Cretaceous turbidite play in the deep-water Ivorian Tano basin is very prolific.

Conclusions

The main findings of this research are:

- Aptian? to late Albian Atlantic continental rifting produced a well-developed rift system in the Ivorian Tano basin. Rift styles include rotated fault blocks and horst & graben structures up to 10 km across.
- The presence of a 'weak' detachment for the rift faults and the low angle dips of these structures may provide evidence of of hyper-extension during rifting.
- Rifting was punctuated by a phase of thermally driven uplift that brought upon a basin-wide phase of erosion of the rift morphology. This thermal event is attributed to the development of the mid-oceanic ridge south of the Ivorian Tano basin during the mid-Albian.
- The transition of the Côte d'Ivoire margin to a full transform margin occurred in the late Albian to Cenomanian with the formation of crustal, oblique-slip faults with 'en echelon' folds at their upper tips.

- Crustal weakening along these large faults controlled the emplacement of the mid to late Albian volcanic centres and sub-volcanic sill complexes.
- This paper shows the first evidence of Albian magmatism in the region as indicated by the well-imaged volcanoes and associated sills at depth.
- In the Cenomanian, a phase of extension formed small scale normal faults which, in places, are linked to rift faults at depth. The tectonic control on this late extensional phase is unclear and may include 'post-rift relaxation' processes or a previously unreported Late Cretaceous regional tectonic event that promoted reactivation of rift faults.
- The variety of stratigraphic and structural features developed through the Cretaceous history of the basin offers high-trapping potentials for a number of plays in the rift as well as in the post-rift sequences.

Acknowledgments

The authors would like to thank CGG Multi-Client and New Ventures for providing the seismic data and permission to publish this paper. Resources and equipment for this research were kindly provided by the Fault Dynamics Research Group. Halliburton are thanked for kindly providing Landmark seismic interpretation software as a University Research Grant. The authors are indebted to Gabor Tari, Ian Davison and Teresa Sabato Ceraldi for their critical review of the manuscript.

References

Antobreh, A.A., Faleide, J.I., Tsikalas, F., Planke, S., 2009. Rift–shear architecture and tectonic development of the Ghana margin deduced from multichannel seismic reflection and potential field data. Mar. Pet. Geol. 26, 345–368. doi:10.1016/j.marpetgeo.2008.04.005

Attoh, K., Brown, L., Guo, J., Heanlein, J., 2004. Seismic stratigraphic record of transpression and uplift on the Romanche transform margin, offshore Ghana. Tectonophysics 378, 1–16. doi:10.1016/j.tecto.2003.09.026

Badley, M.E., Price, J.D. & Backshall, L.C. 1989. Inversion, reactivated faults and related structures: seismic examples from the southern North Sea, in: Cooper, M. A. & Williams, G. D. (eds), Inversion Tectonics, Geological Society Special Publications, 44, 201–219.

Inversion Tectonics. Geological Society, London, Special Publications, 44, 201, https://doi.org/10.1144/GSL.SP.1989.044.01.12.

Bahorich, M., Farmer, S., 1995. The coherence cube. Lead. Edge 14, 1053–1058.

Barnes, A., 2007. A tutorial on complex seismic trace analysis. GEOPHYSICS 72, W33–W43. doi:10.1190/1.2785048

Basile, C., 2015. Transform continental margins — part 1: Concepts and models. Tectonophysics 661, 1–10. doi:10.1016/j.tecto.2015.08.034

Basile, C., Mascle, J., Popoff, M., Bouillin, J.P., Mascle, G., 1993. The Ivory Coast-Ghana transform margin: A marginal ridge structure deduced from seismic data. Tectonophysics 222, 1–19. doi:10.1016/0040-1951(93)90186-N

Bayrakci, G., Minshull, T.A., Sawyer, D.S., Reston, T.J., Klaeschen, D., Papenberg, C., Ranero, C., Bull, J.M., Davy, R.G., Shillington, D.J., Perez-Gussinye, M., Morgan, J.K., 2016. Fault-controlled hydration of the upper mantle during continental rifting. Nat. Geosci. 9, 384–388. doi:10.1038/ngeo2671

Brownfield, M.E., and Charpentier, R.R., 2006, Geology and total petroleum systems of the Gulf of Guinea Province of west Africa: U.S Geological Survey Bulletin 2207-C, 32 p.

Burov, E., Cloetingh, S., 1997. Erosion and rift dynamics: new thermomechanical aspects of post-rift evolution of extensional basins. Earth Planet. Sci. Lett. 150, 7–26. doi:10.1016/S0012-821X(97)00069-1

Burov, E., Poliakov, A., 2003. Erosional forcing of basin dynamics: new aspects of syn-and post-rift evolution, in: Nieuwland,D. A (Ed.), New Insights into Structural Interpretation and Modelling, Geological Society, London, Special Publications, 212, 209–223.

Cartwright, J., Huuse, M., 2005. 3D seismic technology: the geological 'Hubble.' Basin Res. 17, 1–20. doi:10.1111/j.1365-2117.2005.00252.x

Chierici, M.A., 1996. Stratigraphy, palaeoenvironments and geological evolution of the Ivory Coast-Ghana basin. Géologie L'Afrique L'Atlantique Sud Actes Colloq. Angers 1994, 293–303.

Chopra, S., Marfurt, K.J., 2008. Introduction to this special section-Seismic Attributes. Lead. Edge 27, 296–297. doi:10.1190/1.2896619

Chopra, S., Marfurt, K.J., 2007. Seismic attributes for prospect identification and reservoir characterization, Seg Geophysical Developments. Society of Exploration Geophysicists, Tulsa, pp. 464.

Christie-Blick, N., Biddle, K.T., 1985. Deformation and basin formation along strike-slip faults, in: Biddle K. T., Christie-Blick N., (eds) Strike-slip deformation, basin formation, and sedimentation, deformation and basin formation along strike-slip faults, SEPM Special Publications, 37, pp 1–34.

Clift, P.D., Lorenzo, J., Carter, A., Hurford, A.J., Party, O.L. 159 S., 1997. Transform tectonics and thermal rejuvenation on the Côte d'Ivoire-Ghana margin, west Africa. J. Geol. Soc. 154, 483–489. doi:10.1144/gsjgs.154.3.0483

Coole, P., Tyrrell, M., Roche, C., 2015. Offshore Ivory Coast: Reducing Exploration Risk. GeoExpro 12, 80–84.

Cunningham, W.D., Mann, P., 2007. Tectonics of strike-slip restraining and releasing bends, in: Cunningham, W.D., Mann, P., (eds), Tectonics of strike-slip restraining and releasing bends, Geological Society, London, Special Publications, 290, 1–12.

Dailly, P., Henderson, T., Hudgens, E., Kanschat, K., Lowry, P., 2013. Exploration for Cretaceous stratigraphic traps in the Gulf of Guinea, West Africa and the discovery of the Jubilee Field: a play opening discovery in the Tano Basin, Offshore Ghana, in: Mohriak, W. U., Danforth, A., Post, P. J., Brown, D. E., Tari, G. C., Nemčok, M., Sinha, S. T. (eds), Conjugate divergent margins, Geological Society, London, Special Publications, 369, 235–248.

Davison, I., Faull, T., Greenhalgh, J., Beirne, E.O., Steel, I., 2015. Transpressional structures and hydrocarbon potential along the Romanche Fracture Zone: a review, in: Nemčok, M., Rybár, S., Sinha, S. T., Hermeston, S. A., Ledvényiová, L. (eds), Transform margins: development, controls and petroleum systems, Geological Society, London, Special Publications, 431, 235–248.

de Groot, P., Bril, B., 2005. The open source model in geosciences and OpendTect in particular. SEG Technical Program Expanded Abstracts 2005, 802–805. https://doi.org/10.1190/1.2148280.

Doré, T., Lundin, E., 2015. Hyperextended continental margins—Knowns and unknowns. Geology 43, 95–96. doi:10.1130/focus012015.1

Dumestre, M.A., 1985. Northern Gulf of Guinea shows promise. OIL GAS J. 83, 154.

Eagles, G., 2007. New angles on South Atlantic opening. Geophys. J. Int. 168, 353–361.

Elvsborg, A., Dalode, J., 1985. Benin hydrocarbon potential looks promising. Oil Gas J. 6, 126–131.

Firth, J., Horstad, I., Schakel, M., 2014. Experiencing the full bandwidth of energy from exploration to production with the art of BroadSeis. First Break 32, 89–97.

Friedrich, O., Norris, R.D., Erbacher, J., 2012. Evolution of middle to Late Cretaceous oceans—A 55 m.y. record of Earth's temperature and carbon cycle. Geology 40, 107–110. doi:10.1130/G32701.1

Granot, R., Dyment, J., 2015. The Cretaceous opening of the South Atlantic Ocean. Earth Planet. Sci. Lett. 414, 156–163. doi:10.1016/j.epsl.2015.01.015

Haack, R. C., P. Sundararaman, J. O. Diedjomahor, H. Xiao, N. J. Gant, E. D. May, and K. Kelsch, 2000. Niger Delta petroleum systems, Nigeria, in: M. R. Mello and B. J. Katz, (eds), Petroleum systems of South Atlantic margins, AAPG Memoir 73, 213–231.

Hansen, D.Mø., Cartwright, J.A., Thomas, D., 2004. 3D Seismic Analysis of the Geometry of Igneous Sills and Sill Junction Relationships, in: Davies, R. J., Cartwright, J. A, Stewart, S. A., Lappin, M., Underhill, J. R. (eds), 3D Seismic technology: application to the exploration of sedimentary basins, Geological Society, London, Memoirs, 29, 199–208.

Heine, C., Zoethout, J., Müller, R.D., 2013. Kinematics of the South Atlantic rift. Solid Earth 4, 215–253. doi:10.5194/se-4-215-2013

Hill, D., Combee, C., Bacon, J., 2006. Over/under acquisition and data processing: the next quantum leap in seismic technology? First Break, 24, 81–96.

Holmes, M.A., 1998. Thermal diagenesis of Cretaceous sediment recovered at the Côte d'Ivoire Ghana Transform Margin, in: Mascle, J., Lohmann, G.P., Moullade, M. (Eds.), Proceedings of the Ocean Drilling Program, Scientific Results. College Station, Texas, pp. 53–70.

Iacopini, D., Butler, R.W.., 2011. Imaging deformation in submarine thrust belts using seismic attributes. Earth Planet. Sci. Lett. 302, 414–422.

Jones, E.J.W., Cande, S.C., Spathopoulos, F., 1995. Evolution of a major oceanographic pathway: the equatorial atlantic, in: Scrutton, R. A., Stoker, M. S, Shimmield, G. B., Tudhope, A. W. (eds.), The Tectonics, Sedimentation and Palaeoceanographyof the North Atlantic Region, Special Publication. Geological Society, London, 90, 199–213.

Kelley, D.S., Baross, J.A., Delaney, J.R., 2002. Volcanoes, Fluids, and Life at Mid-Ocean Ridge Spreading Centers. Annu. Rev. Earth Planet. Sci. 30, 385–491. doi:10.1146/annurev.earth.30.091201.141331

Kjemperud, A., Agbesinyale, W., Agdestein, T., Gustafsson, C., Yükler, A., 1991. Tectono-stratigraphic history of the Keta basin, Ghana with emphasis on late erosional episodes. Géologie Afr. Coll Géol Libr. Recl. Commun. 55–69.

MacGregor, D.S., Robinson, J., Spear, G., 2003. Play fairways of the Gulf of Guinea transform margin, in: Arthur, T. J., MacGregor, D. S., Cameron, N. R. (eds), Petroleum geology of Africa: new themes and developing technologies, Geological Society, London, Special Publications, 207, 131–150.

Marfurt, K.J., Alves, T.M., 2015. Pitfalls and limitations in seismic attribute interpretation of tectonic features. Interpretation 3, SB5-SB15. doi:10.1190/INT-2014-0122.1

Marfurt, K.J., Kirlin, R.L., Farmer, S.L., Bahorich, M.S., 1998. 3-D seismic attributes using a semblance-based coherency algorithm. Geophysics 63, 1150–1165.

Martin, J., Duval, G., Lamourette, L., 2015. What Lies Beneath the Deepwater Tano Basin. GeoExpro 12, 28–30.

Mascle, J., Blarez, E., 1987. Evidence for transform margin evolution from the Ivory Coast–Ghana continental margin. Nature 326, 378–381. doi:10.1038/326378a0

McClay, K.R., 1990. Extensional fault systems in sedimentary basins: a review of analogue model studies. Mar. Pet. Geol. 7, 206–233. doi:10.1016/0264-8172(90)90001-W

McClay, K.R., Ellis, P.G., 1987. Geometries of extensional fault systems developed in model experiments. Geology 15, 341–344. doi:10.1130/0091-7613(1987)15<341:GOEFSD>2.0.CO;2

Mercier de Lépinay, M., Loncke, L., Basile, C., Roest, W.R., Patriat, M., Maillard, A., De Clarens, P., 2016. Transform continental margins – Part 2: A worldwide review. Tectonophysics 693, Part A, 96–115. doi:10.1016/j.tecto.2016.05.038

Morgan, P., 1983. Constraints on rift thermal processes from heat flow and uplift. Tectonophysics, Processes of Continental Rifting 94, 277–298. doi:10.1016/0040-1951(83)90021-5

Morrison, J., Burgess, C., Cornford, C., N'Zalasse, B., 2000. Hydrocarbon systems of the Abidjan margin, Côte d'Ivoire. Offshore West Africa, Fourth Annual Conference, Abidjan, 21-23 March 2000. Pennwell Publishing, Tulsa, Oklahoma.

Moulin, M., Aslanian, D., Unternehr, P., 2010. A new starting point for the South and Equatorial Atlantic Ocean. Earth-Sci. Rev. 98, 1–37. doi:10.1016/j.earscirev.2009.08.001

Nemčok, M., Henk, A., Allen, R., Sikora, P.J., Stuart, C., 2013. Continental break-up along strike-slip fault zones; observations from the Equatorial Atlantic, in: Mohriak, W.U., Danforth, W.U., Post, P.J., Brown, D. E., Tari, G. C., Nemčok, M., Sinha, S. T. (eds), Conjugate divergent margins, Geological Society, London, Special Publications, 369, 537–556.

Nemčok, M., Rybár, S., Sinha, S.T., Hermeston, S.A., Ledvényiová, L., 2016. Transform margins: development, controls and petroleum systems, Geological Society Special Publication, 431, The Geological Society, London, pp. 385.

Nürnberg, D., Müller, R.D., 1991. The tectonic evolution of the South Atlantic from Late Jurassic to present. Tectonophysics 191, 27–53.

Peirce, C., Whitmarsh, R.B., Scrutton, R.A., Pontoise, B., Sage, F., Mascle, J., 1996. Côte d'Ivoire-Ghana margin: seismic imaging of passive rifted crust adjacent to a transform continental margin. Geophys. J. Int. 125, 781–795. doi:10.1111/j.1365-246X.1996.tb06023.x

Pérez-Díaz, L., Eagles, G., 2014. Constraining South Atlantic growth with seafloor spreading data. Tectonics, 33, 1848–1873, doi:10.1002/2014TC003644

Pletsch, T., Erbacher, J., Holbourn, A.E.L., Kuhnt, W., Moullade, M., Oboh-Ikuenobede, F.E., Söding, E., Wagner, T., 2001. Cretaceous separation of Africa and South America: the view from the West African margin (ODP Leg 159). J. South Am. Earth Sci., Mesozoic Palaeontology and Stratigraphy of South America and the South Atlantic 14, 147–174. doi:10.1016/S0895-9811(01)00020-7

Posamentier, H.W., Davies, R.J., Cartwright, J.A., Wood, L., 2007. Seismic geomorphology - an overview, in: Davies, R. J., Posamentier, H. W., Wood, L. J. (eds), Seismic Geomorphology: Applications to Hydrocarbon Exploration and Production, Geological Society, London, Special Publications, 227, 1–14.

Rabinowitz, P.D., LaBrecque, J., 1979. The Mesozoic South Atlantic Ocean and evolution of its continental margins. J. Geophys. Res. 84, 5973–6002.

Ranero, C.R., Pérez-Gussinyé, M., 2010. Sequential faulting explains the asymmetry and extension discrepancy of conjugate margins. Nature 468, 294–299. doi:10.1038/nature09520

Reston, T.J., Pérez-Gussinyé, M., 2007. Lithospheric extension from rifting to continental breakup at magma-poor margins: rheology, serpentinisation and symmetry. Int J Earth Sci (Geol Rundsch) 96, 1033–1046. doi:10.1007/s00531-006-0161-z

Sabato Ceraldi, T., Hodgkinson, R., Backé, G., 2016. The petroleum geology of the West Africa margin: an introduction, Geological Society Special Publication, 438, The Geological Society, London, pp. 228

Sage, F., Basile, C., Mascle, J., Pontoise, B., Whitmarsh, R.B., 2000. Crustal structure of the continent–ocean transition off the Côte d'Ivoire–Ghana transform margin: implications for thermal exchanges across the palaeotransform boundary. Geophys. J. Int. 143, 662–678. doi:10.1046/j.1365-246X.2000.00276.x

Sandwell, D.T., Müller, R.D., Smith, W.H.F., Garcia, E., Francis, R., 2014. New global marine gravity model from CryoSat-2 and Jason-1 reveals buried tectonic structure. Science 346, 65–67. doi:10.1126/science.1258213

Sinton, J.M., Detrick, R.S., 1992. Mid-ocean ridge magma chambers. J. Geophys. Res. Solid Earth 97, 197–216. doi:10.1029/91JB02508

Tari, G. 2006. Traditional and new play types of the offshore Tano Basin of Côte D'Ivoire and Ghana, West Africa. Houston Geological Society Newsletter, January, 48, 27–34.

Torsvik, T.H., Rousse, S., Labails, C., Smethurst, M.A., 2009. A new scheme for the opening of the South Atlantic Ocean and the dissection of an Aptian salt basin. Geophys. J. Int. 177, 1315–1333.

Wells, S., Warner, M., Greenhalgh, J., Borsato, R., 2012. Offshore Côte d'Ivoire: A Modern Exploration Frontier. GeoExpro 9, 36–40.

Ye, J., Chardon, D., Rouby, D., Guillocheau, F., Dall'asta, M., Ferry, J.-N., Broucke, O., 2017. Paleogeographic and structural evolution of northwestern Africa and its Atlantic margins since the early Mesozoic. Geosphere, 13, 1–31

Figure Captions

Figure. 1. Location maps of the study area.

a) Vertical gravity gradient map derived from Bouguer gravity data showing the location of the Ivorian Tano Basin along the West Africa equatorial margin. Note that the basin is bounded by two large fracture zones, the St. Paul to the north and the Romanche to the south. Data from Sandwell et al. (2014).

b) Bathymetric map with major faults highlighted and showing the location of the 3D seismic data analysed in this study. The data is a subset (yellow dashed line) of a larger volume (grey shade) acquired by CGG in 2014. Main basin features outlined from this work, from Dailly et al. (2013) and from Basile et al. (1993).

Figure 2. Tectono-stratigraphic chart of the Ivorian Tano Basin compiled from results of this work and from Kjemperud et al. (1991), MacGregor et al. (2003) Brownfield & Charpentier (2006) and Wells et al. (2012).

Figure 3. Regional geo-section across the Ivorian Tano basin showing the architecture of the Côte d'Ivoire margin. The section is compiled from results of this research and from Brownfield & Charpentier (2006).

Figure 4. Seismo-stratigraphic diagram illustrating the main seismic horizons interpreted in this study. This is focused at depths of 5–11 km where deep stratigraphic units offset by faults are clearly imaged on amplitude and reflection strength displays.

Figure 5. Key NE–SW section across the 3D survey showing the main structural and stratigraphic features observed in the study area. Note to the NE the presence of a well-developed extensional fault system affecting the Aptian–Albian sequences. Aptian–Albian faulted strata together with Cenomanian and younger units are folded by prominent ridges. Also note that to the SW an extensive igneous complex and an associated volcanic system are clearly imaged. Section location is shown in Figure 1.

Figure 6. Depth structure map of the Mid Albian horizon. The map shows that the mid-Albian strata are affected by a series NW–SE trending extensional faults. The faults exhibit various structural styles, including half-graben structures, horst & graben structures, as well as domino style faults blocks. Interpretation of the horizon was achieved in the eastern part of the dataset, where imaging of this deep section was not affected by magmatic intrusions as shown in Figures 5 & 12b.

Figure 7. Uninterpreted and interpreted section showing Aptian? to Albian strata affected by a series of NE-dipping extensional faults. The fault dips are shallowly dipping at 20-35º and delineate highly rotated fault blocks up to 10 km across (cf. Fig. 8). Shallow fault dips and marked rotation of faulted strata indicate high level of extension above a low angle, weak detachment surface.

Figure 8. Uninterpreted and interpreted section showing a horst & graben structure in Aptian?–Albian strata. The horst bounding faults are listric and are interpreted to

terminate at depth onto a common low-angle detachment unit. Note that hangingwall strata to the NE clearly exhibit up to 2 km of fanning growth strata of possible Aptian-Albian age. These indicate long-lived extension until the end of the Albian. Evidence of erosional truncations below the Mid Albian horizon (cf. Fig. 7) may indicate two distinct phases of extension.

Figure 9. a) Depth structure map; b) Dip-steered coherency extraction of Top Albian horizon; c) Structure map with orientation of the main features described shown in the inset rose diagram. Note in panel ‘a’ a series of prominent SW–NE-trending folds. In the same panel, three volcanic complexes also occur. A set of well-developed normal faults with a NNW–SSE orientation are clearly imaged in the coherency extraction shown in panel ‘b’. Details of these two sets of structures are presented in Figure 10a.

Figure 10. a) Detailed 3D view of Top Albian horizon showing folds and faults affecting this unit;

b) Uninterpreted and interpreted detailed sections through key folds. The locations of these sections are shown in panel ‘a’. Note in panel ‘a’ the presence of numerous faults that offset and therefore postdate the ridges. The sections in panel ‘b’ show that the ridges are markedly asymmetric, an indication that these may be associated with faults at depth. Stratal terminations and thickness variations across the fold in the Albian–Cenomanian intervals indicate active folding occurring at that time. Parallel packages of Turonian and younger stratigraphy form drape units that seal the folds. Also, note the ‘en echelon’ arrangement of the ridges observed in panel ‘a’ possible evidence of oblique slip along the faults present in the core of these structures.

Figure 11. Uninterpreted and interpreted detailed section showing planar faults affecting Albian–Cenomanian strata. These show limited displacement which hinders the recognition of clear growth strata. The upper tips of the faults clearly offset the Top Albian horizon, whereas the Top Cenomanian appears unaffected. This indicates the faults were short lived, with active faulting at the transition between the Albian and Cenomanian. Some sections also show that these faults may have formed because of reactivation of older faults as observed in Figure 8.

Figure 12. a) Seismic block diagram showing a well-developed magmatic plumbing system in the study area. The block is cropped at the Top Cenomanian horizon and shows three volcanic edifices with a series of sills at depth.

b) Reflection strength extraction at a depth of 7.5 km showing the extent of the sill complexes. These extend over distances in excess of 70 km and developed around the volcanic edifices – in this extraction the magma conduits are imaged as circular features with a low strength response (see also Fig. 13).

c) Co-displayed geobodies and reflection strength in vertical section. The geobodies were constructed to map the high amplitudes associated with the sill complexes as seen on the reflection strength displays. Individual sills vary in shape and dimension from strata-concordant to saucer-shaped intrusions which can extend laterally for up to 8 km.

Figure 13. a) Uninterpreted b) reflection strength and b) interpreted section showing a key example of a volcanic edifice in the study area. The surface delineating the top of the volcano (Top Volcano) is defined by a series of onlap terminations of Cenomanian and younger strata. Below this surface, a well-developed volcano stratigraphy can be recognised in the form of packages of continuous reflections of variable amplitudes dipping away from the summit and downlapping onto the paleo-depositional surface at the time of extrusion (Base Volcano). These stratal relationships indicate that volcanism mainly occurred in the late Albian. The reflection strength display highlights the presence of a number of sill intrusions at depth as well as a disrupted, low amplitude columnar zone below the volcanic edifice and may indicate the main magma conduit.

Figure 14. a) An event chart compiled from the seismic analysis shown this study. b) Summary rose diagrams showing main orientations of structures identified in this research.

Figure 15. Schematic evolutionary model of the Ivorian Tano basin during the Aptian–Cenomanian.

a) Aptian–Albian rifting.

b) Continued rifting through the Albian, with a spreading centre formed to the south. Shearing along the newly formed Romanche Fracture Zone produced deformation and associated magmatism in the basin.

c) Cenomanian, initiation of seafloor spreading contiguous with the basin evolution with eastward migration. The basin slid past the southern spreading centre and became part of tectonically inactive passive transform margin.

Figure1a

Click here to download Figure Figure01a.png

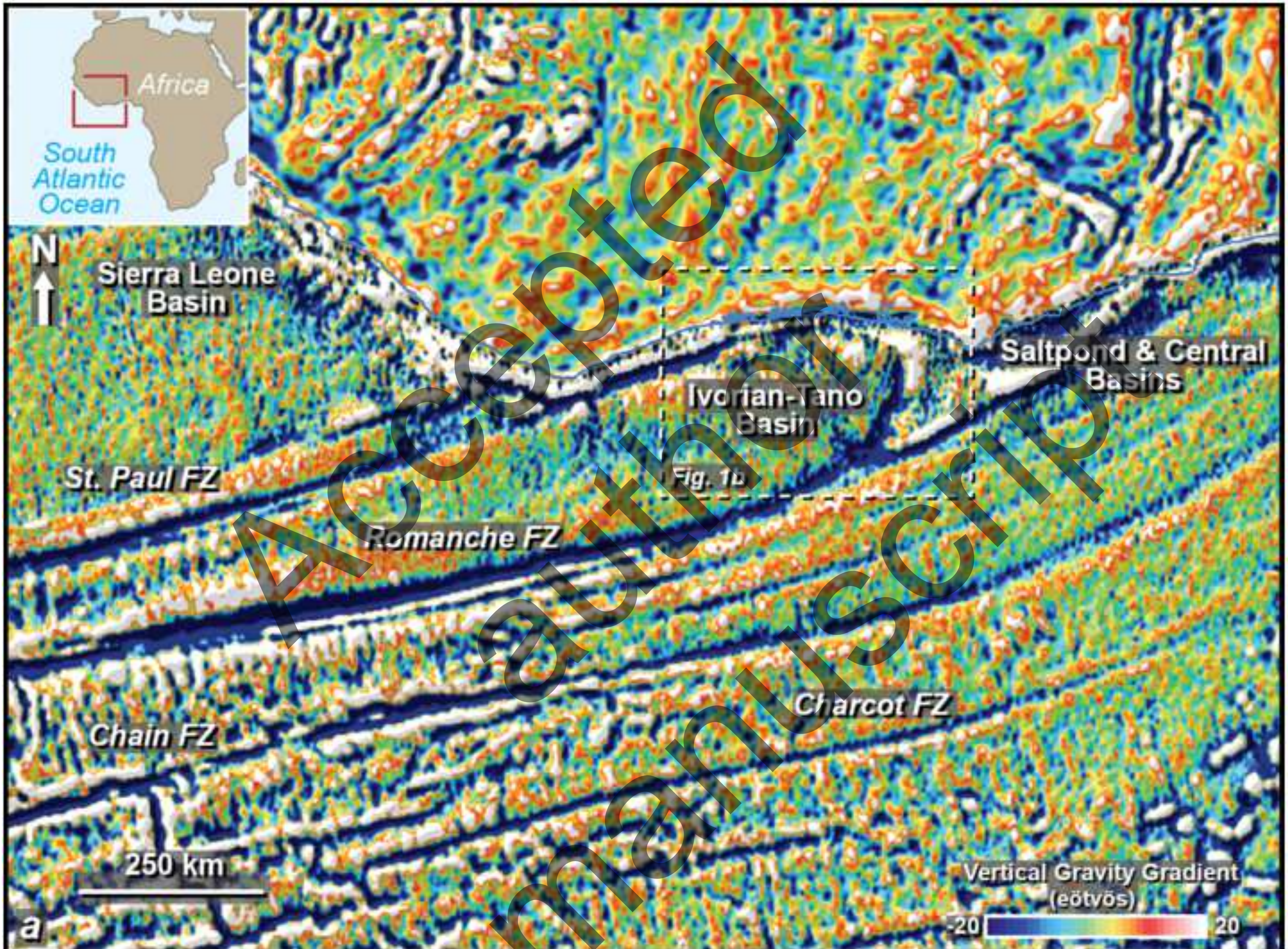

Figure01b

Click here to download Figure Figure01b.png

Figure02 Click here to download Figure Figure02.png

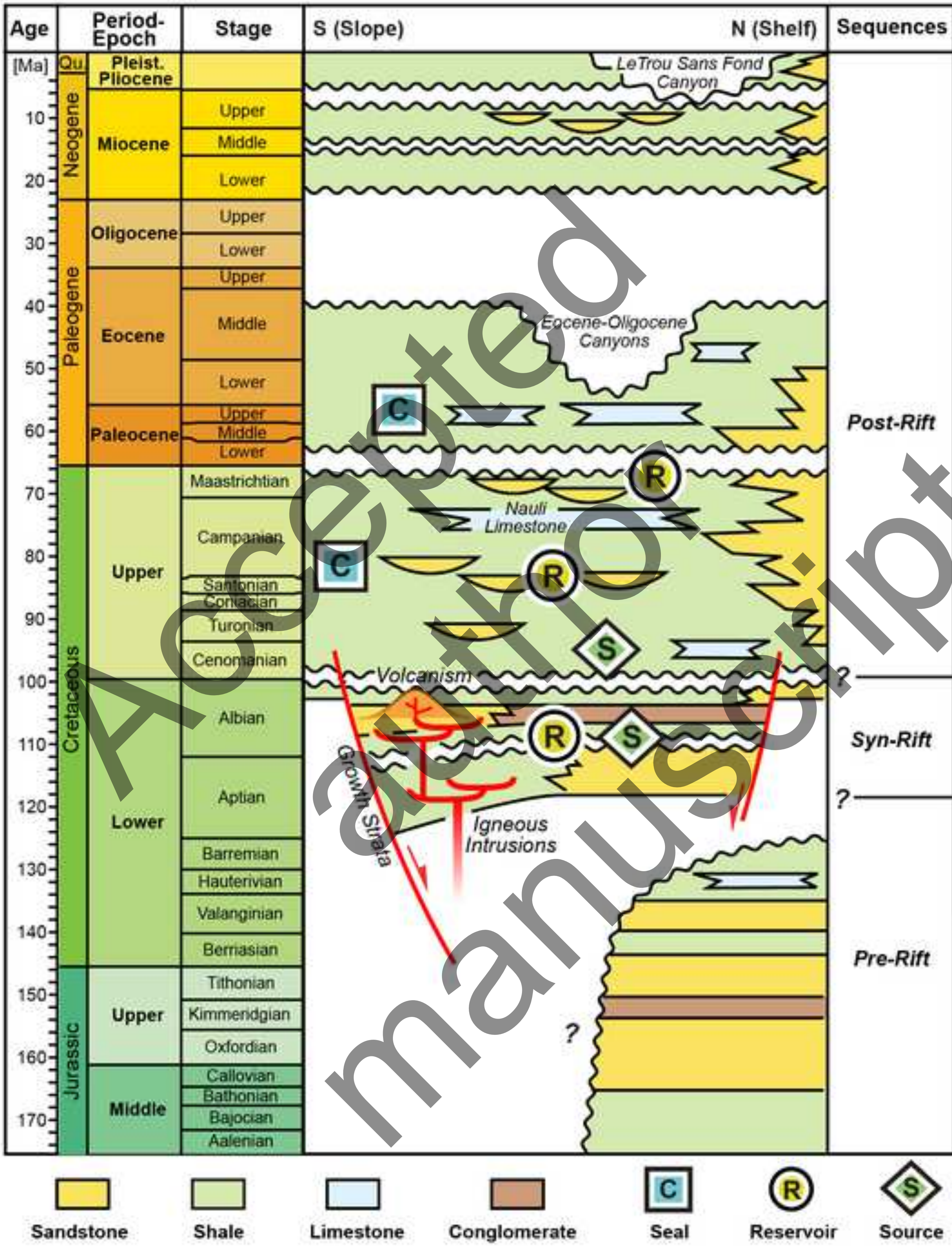

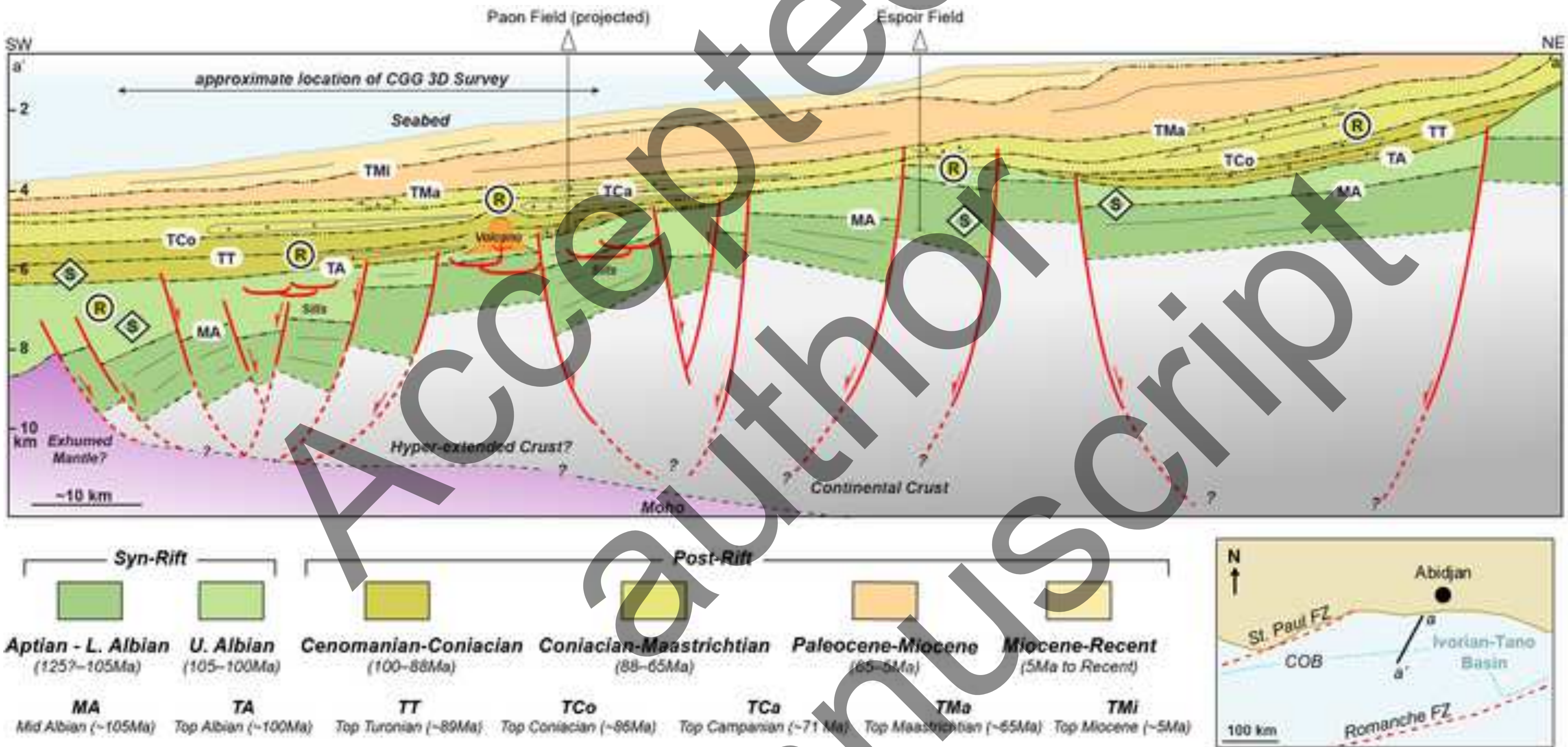
Paon Field (projected)
Espoir Field
SW
NE
approximate location of CGG 3D Survey
Seabed
TMi
TMa
TCa
TCo
TT
TA
MA
Volcano
Sills
Exhumed Mantle?
Hyper-extended Crust?
Continental Crust
Moho
~10 km
Syn-Rift
Post-Rift
Aptian - L. Albian
(125?–105Ma)
U. Albian
(105–100Ma)
Cenomanian-Coniacian
(100–88Ma)
Coniacian-Maastrichtian
(88–65Ma)
Paleocene-Miocene
(65–5Ma)
Miocene-Recent
(5Ma to Recent)
MA
Mid Albian (~105Ma)
TA
Top Albian (~100Ma)
TT
Top Turonian (~89Ma)
TCo
Top Coniacian (~86Ma)
TCa
Top Campanian (~71 Ma)
TMa
Top Maastrichtian (~65Ma)
TMi
Top Miocene (~5Ma)
N
Abidjan
St. Paul FZ
COB
Ivorian-Tano Basin
Romanche FZ
100 km

Figure4

Click here to download Figure Figure04.png

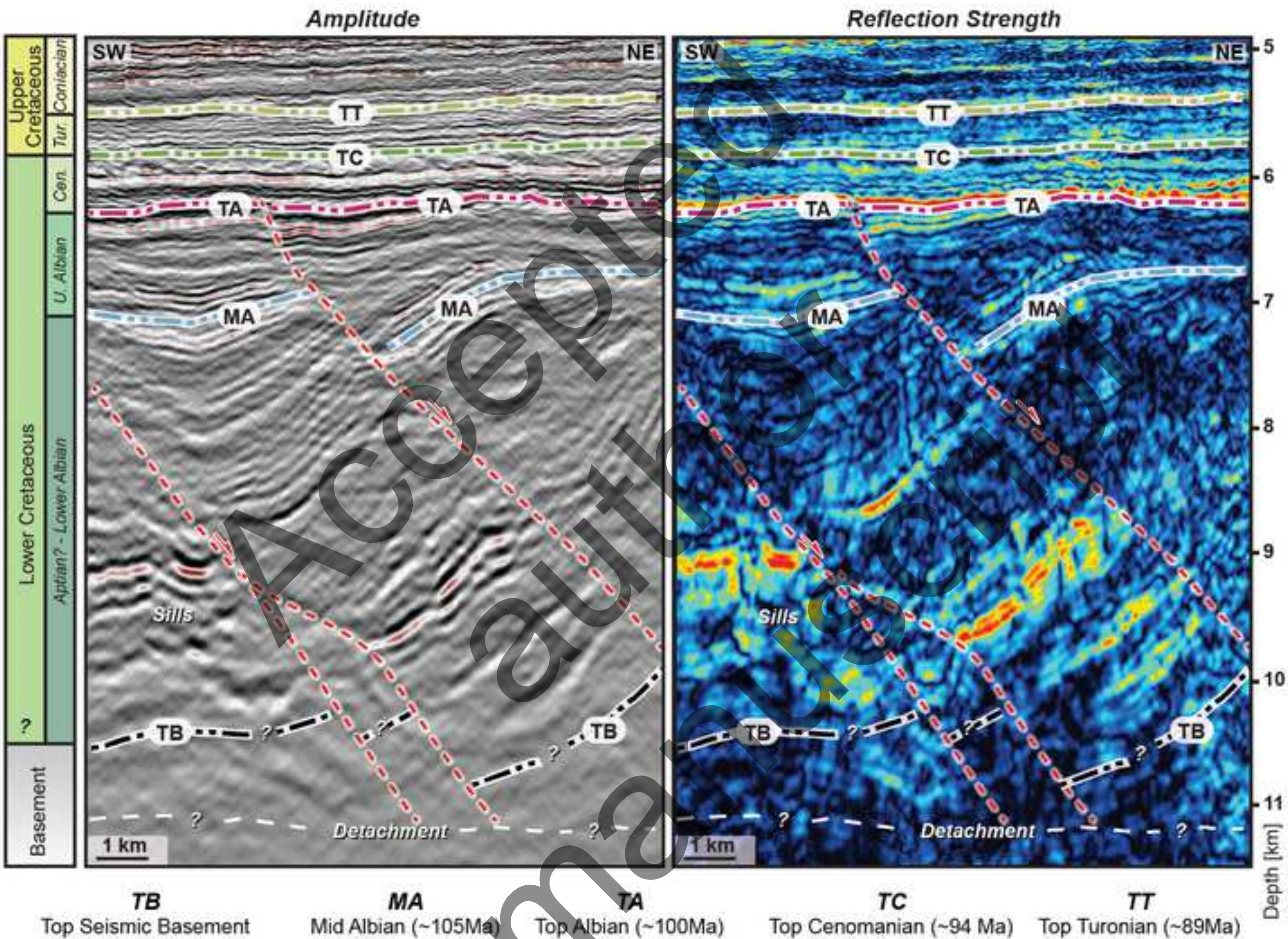

Figure5

Click here to download Figure Figure05.png

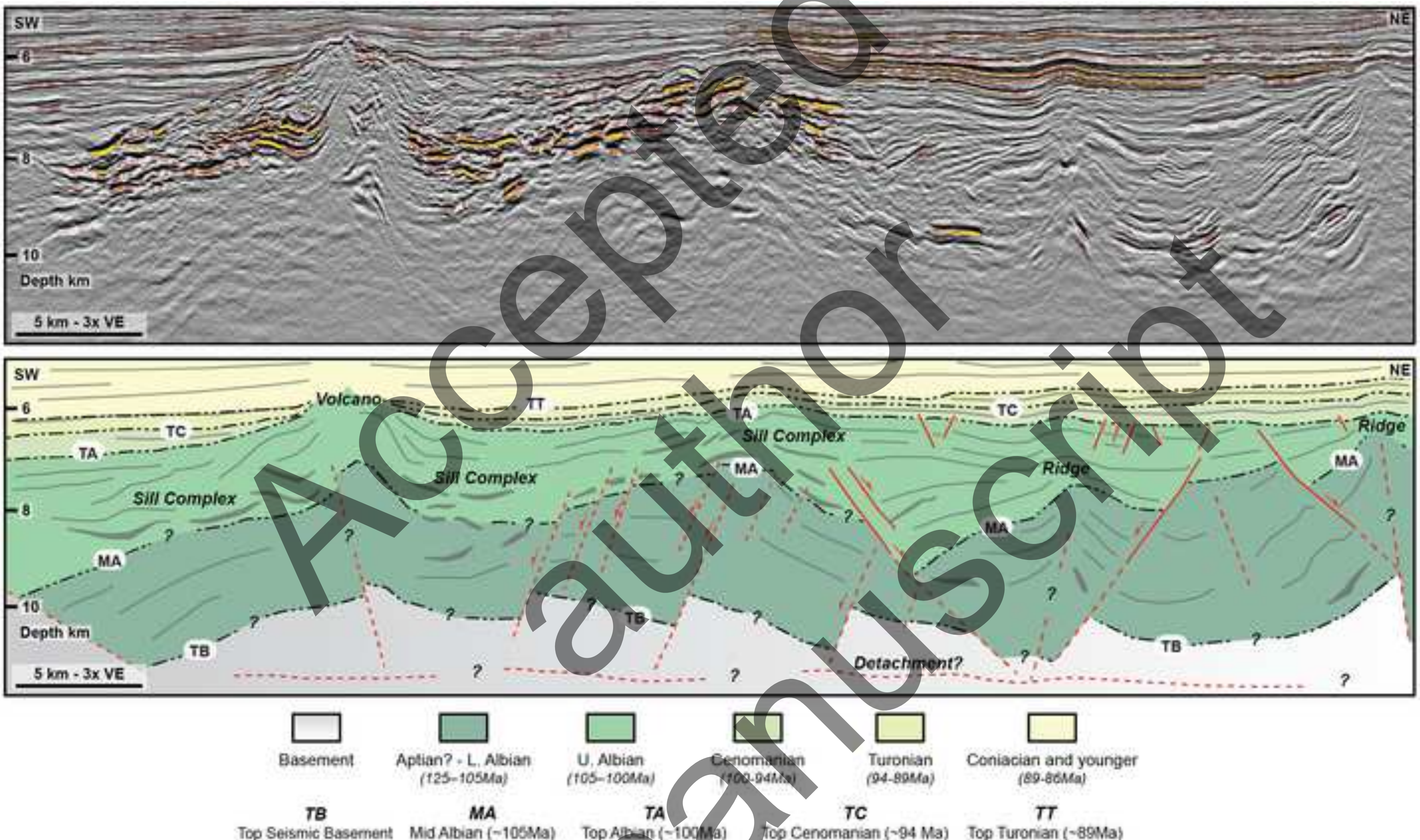

Figure6

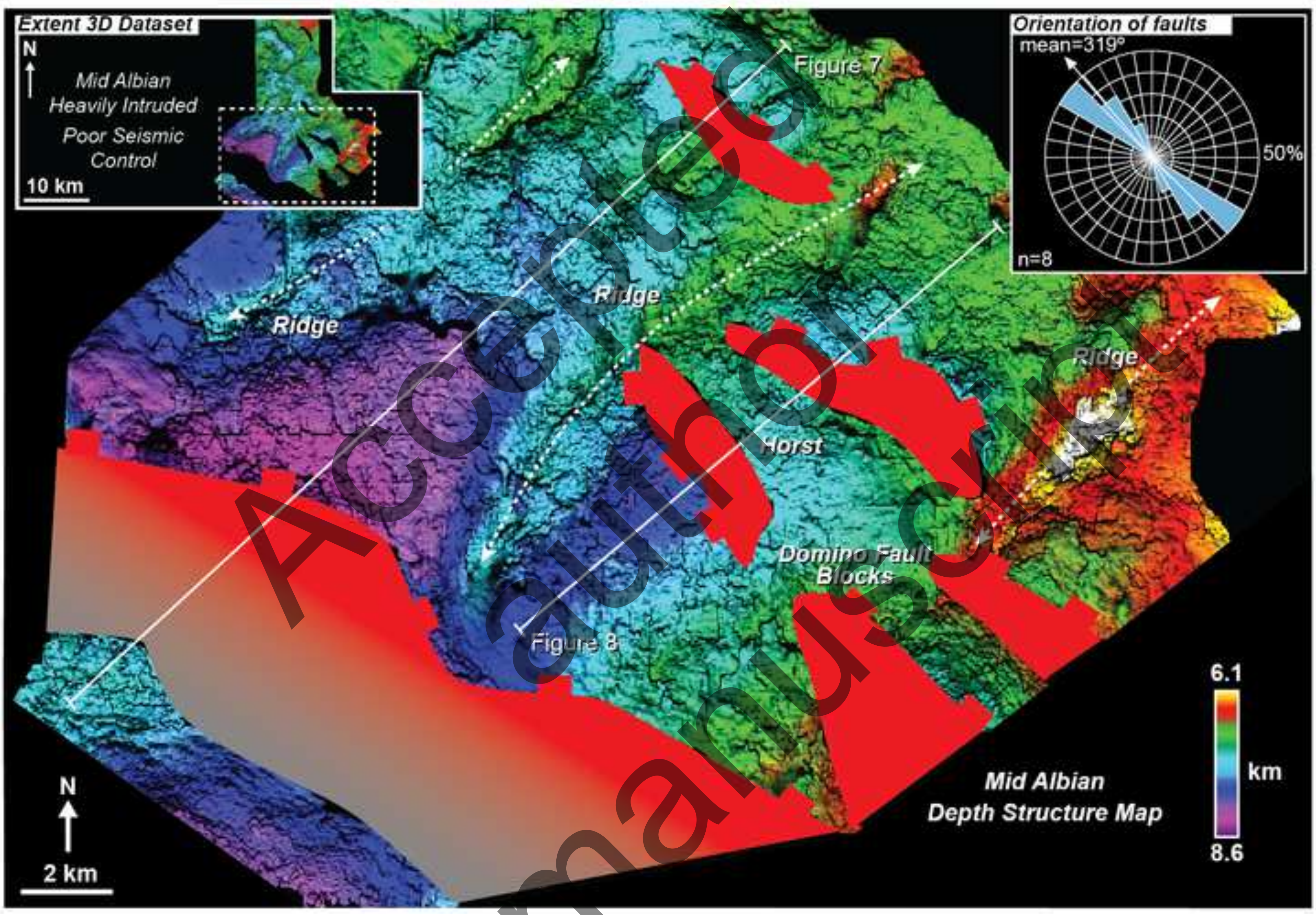
Extent 3D Dataset
N
Mid Albian
Heavily Intruded
Poor Seismic
Control
10 km
Orientation of faults
mean=319°
50%
n=8
Figure 7
Ridge
Ridge
Ridge
Horst
Domino Fault
Blocks
Figure 8
N
2 km
Mid Albian
Depth Structure Map
6.1
km
8.6

Figure7

Click here to download Figure Figure07.png

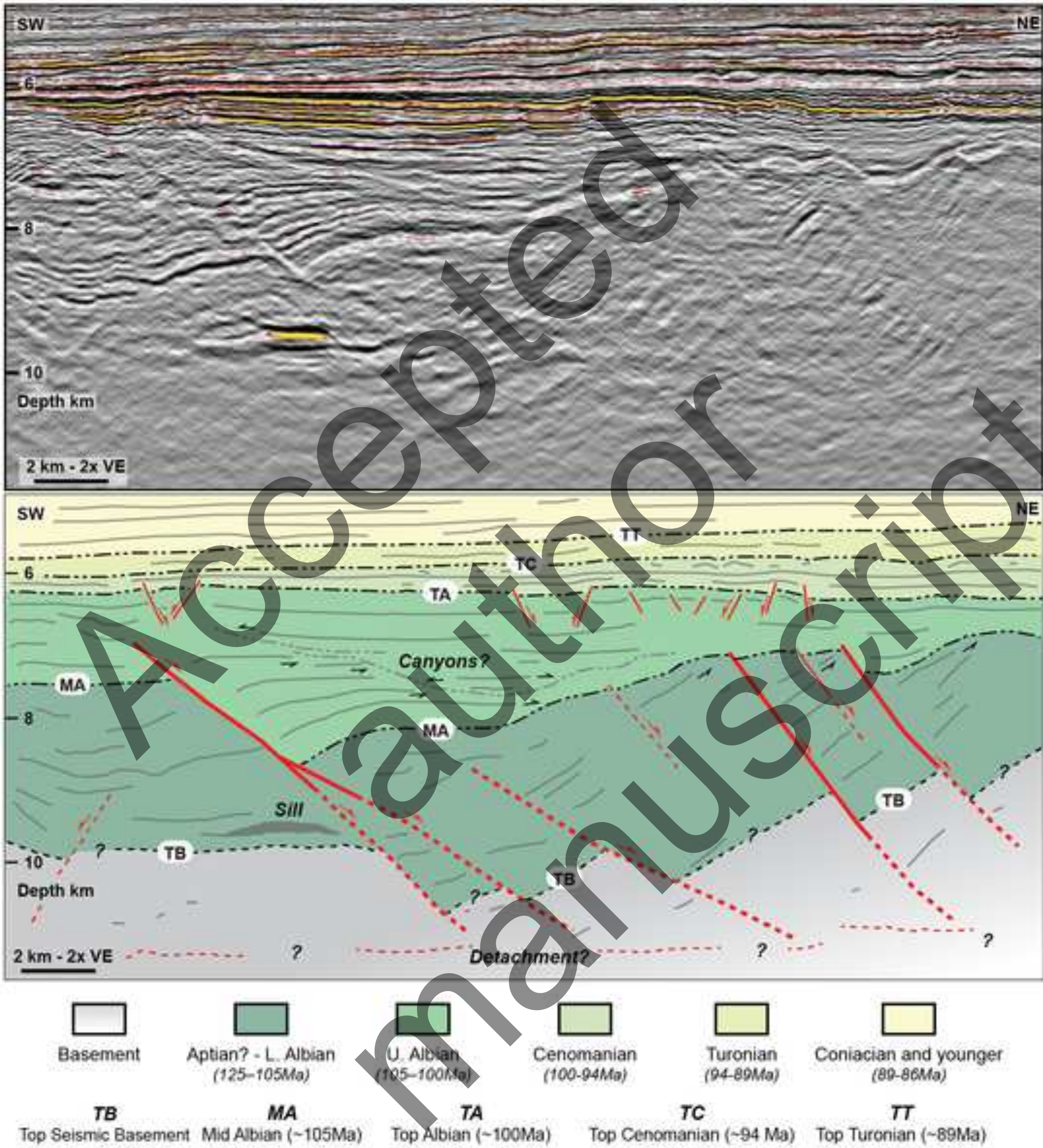

Figure8

Click here to download Figure Figure08.png

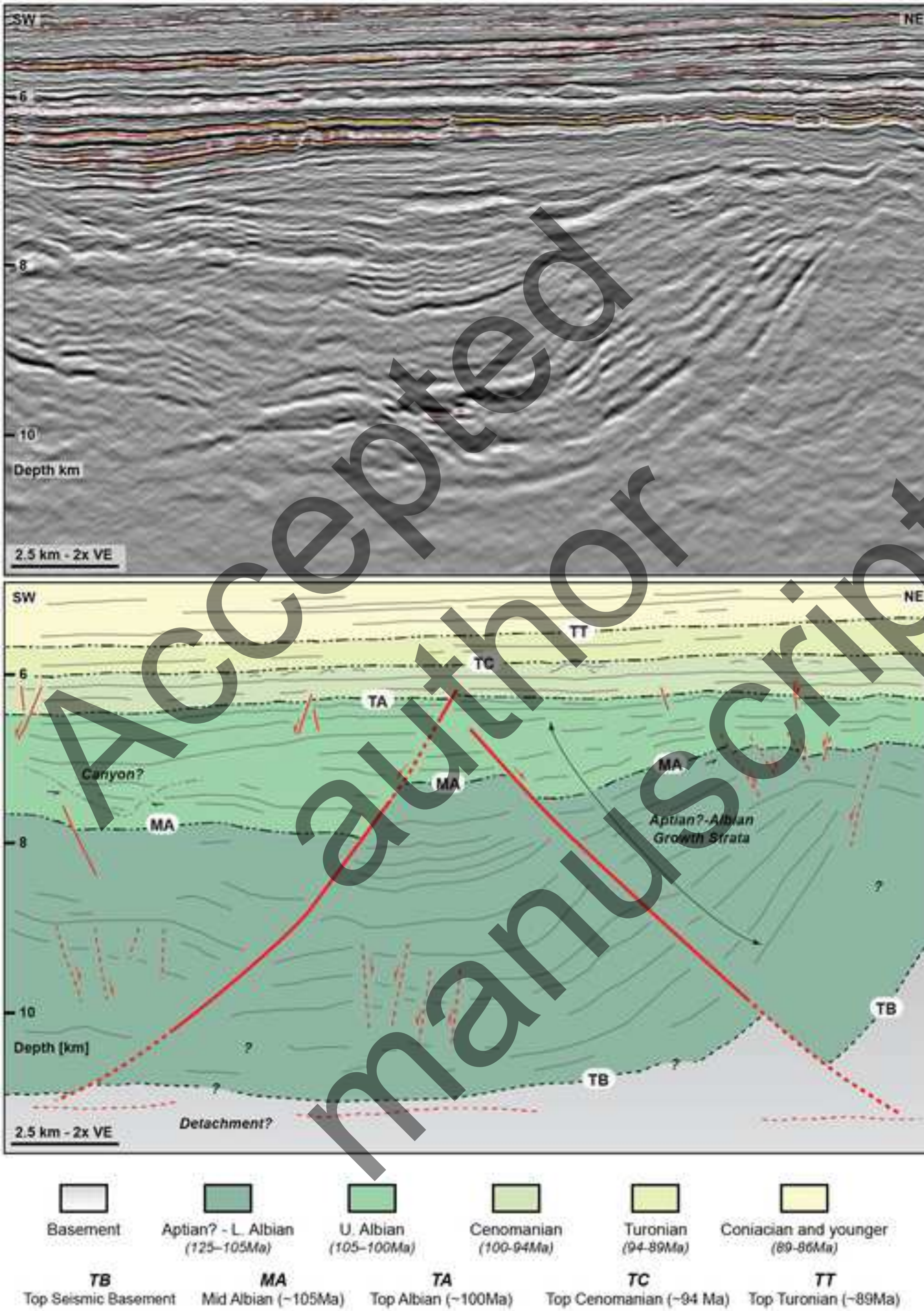

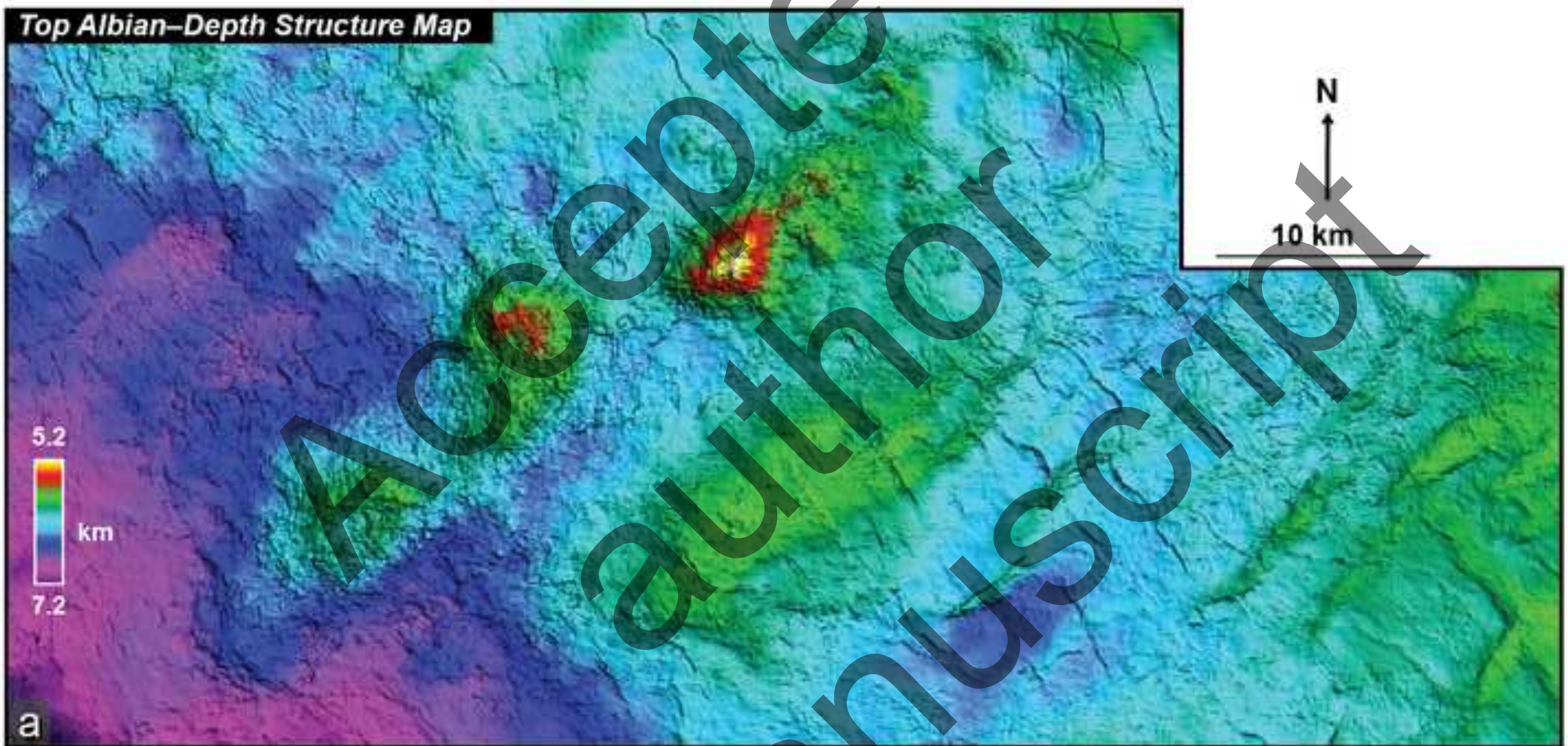
Top Albian–Depth Structure Map
N
10 km
5.2
km
7.2
a

Figure9b

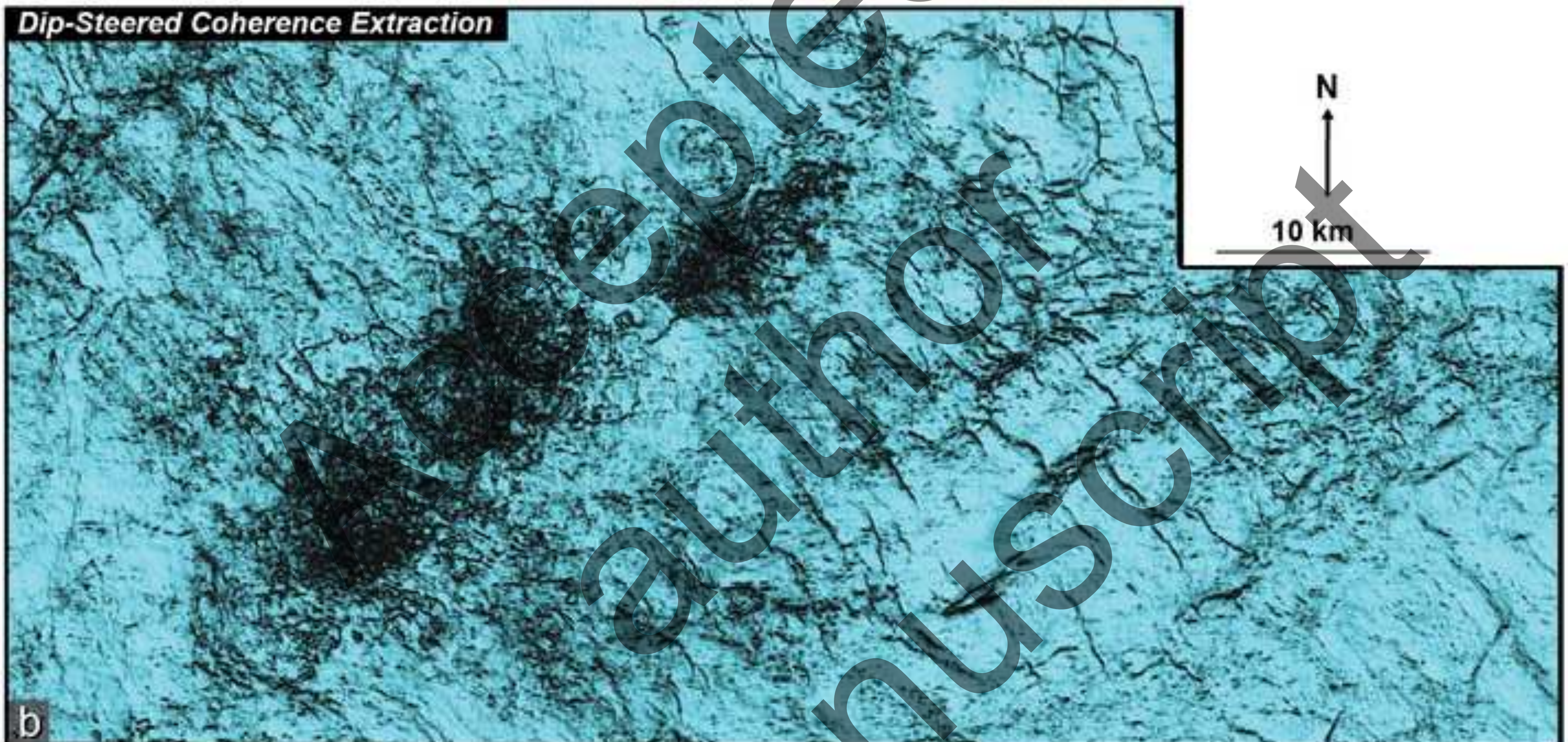

Figure9c

Click here to download Figure Figure09c.png

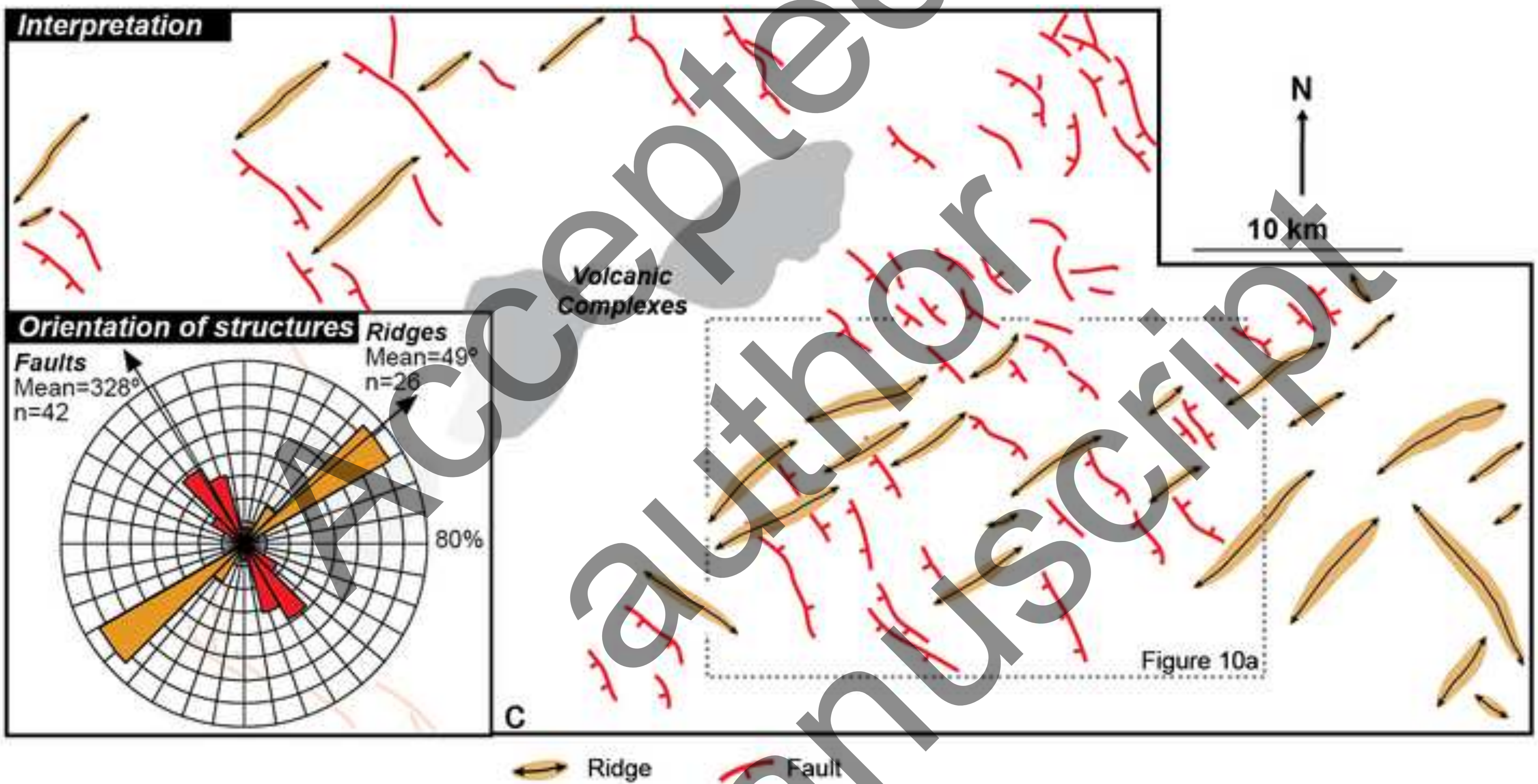

Figure10a

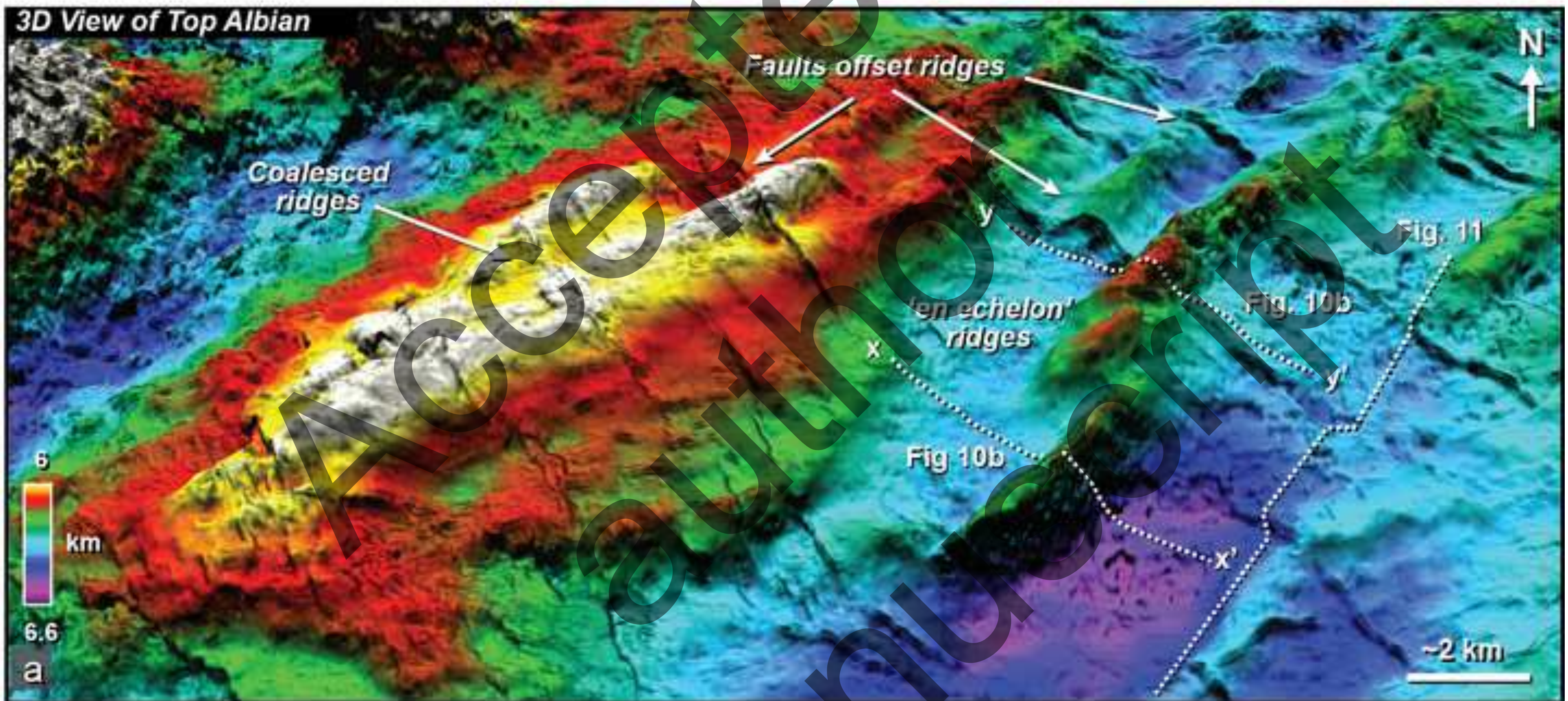
3D View of Top Albian
Faults offset ridges
Coalesced ridges
N
y
'en echelon' ridges
x
Fig. 11
Fig. 10b
y'
Fig 10b
x'
6
km
6.6
a
~2 km

Figure10b

Click here to download Figure Figure10b.png

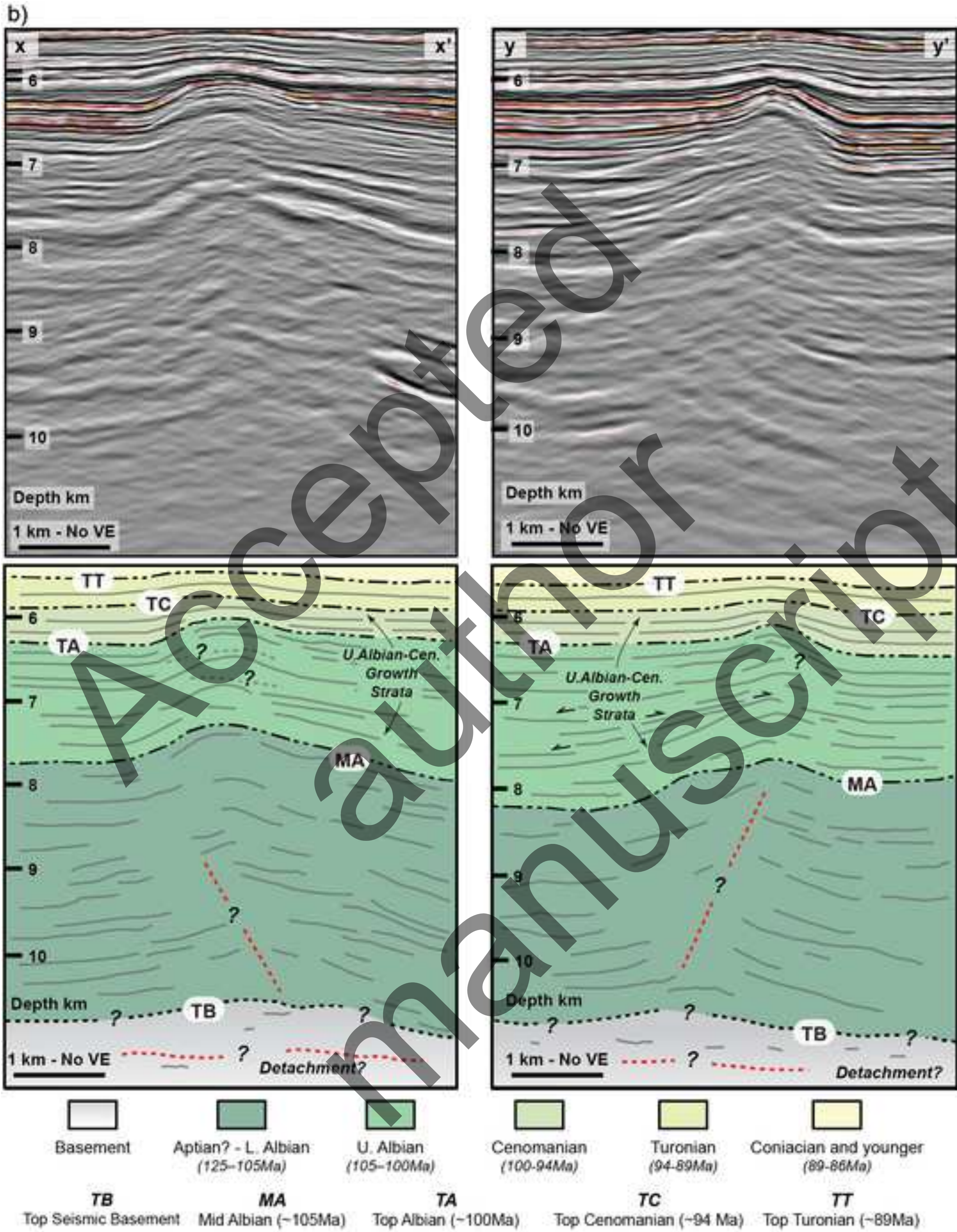

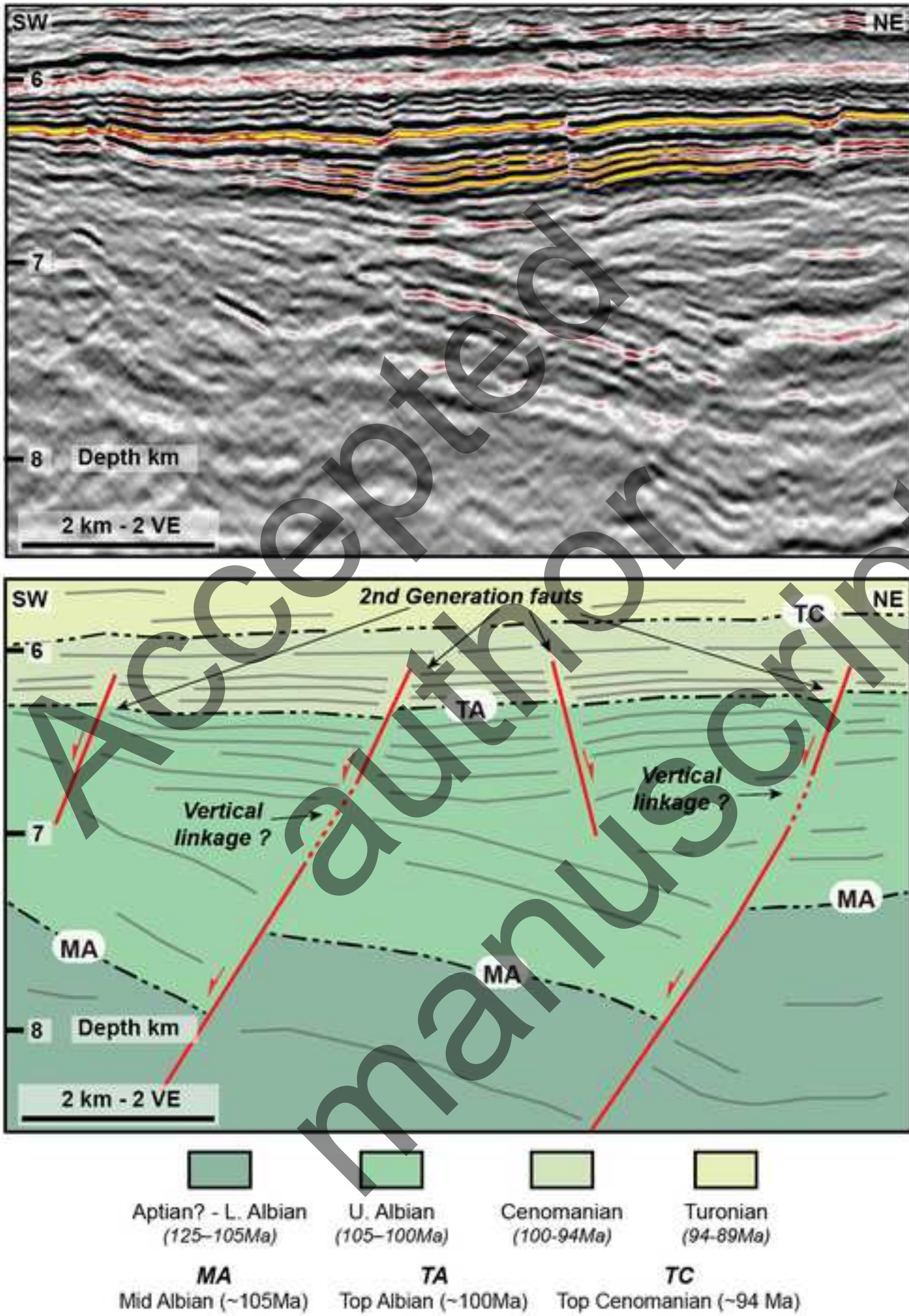
SW
NE
6
7
8
Depth km
2 km - 2 VE
SW
NE
2nd Generation fauts
TC
6
TA
Vertical linkage ?
Vertical linkage ?
7
MA
MA
MA
8
Depth km
2 km - 2 VE
Aptian? - L. Albian
(125–105Ma)
U. Albian
(105–100Ma)
Cenomanian
(100-94Ma)
Turonian
(94-89Ma)
MA
Mid Albian (~105Ma)
TA
Top Albian (~100Ma)
TC
Top Cenomanian (~94 Ma)

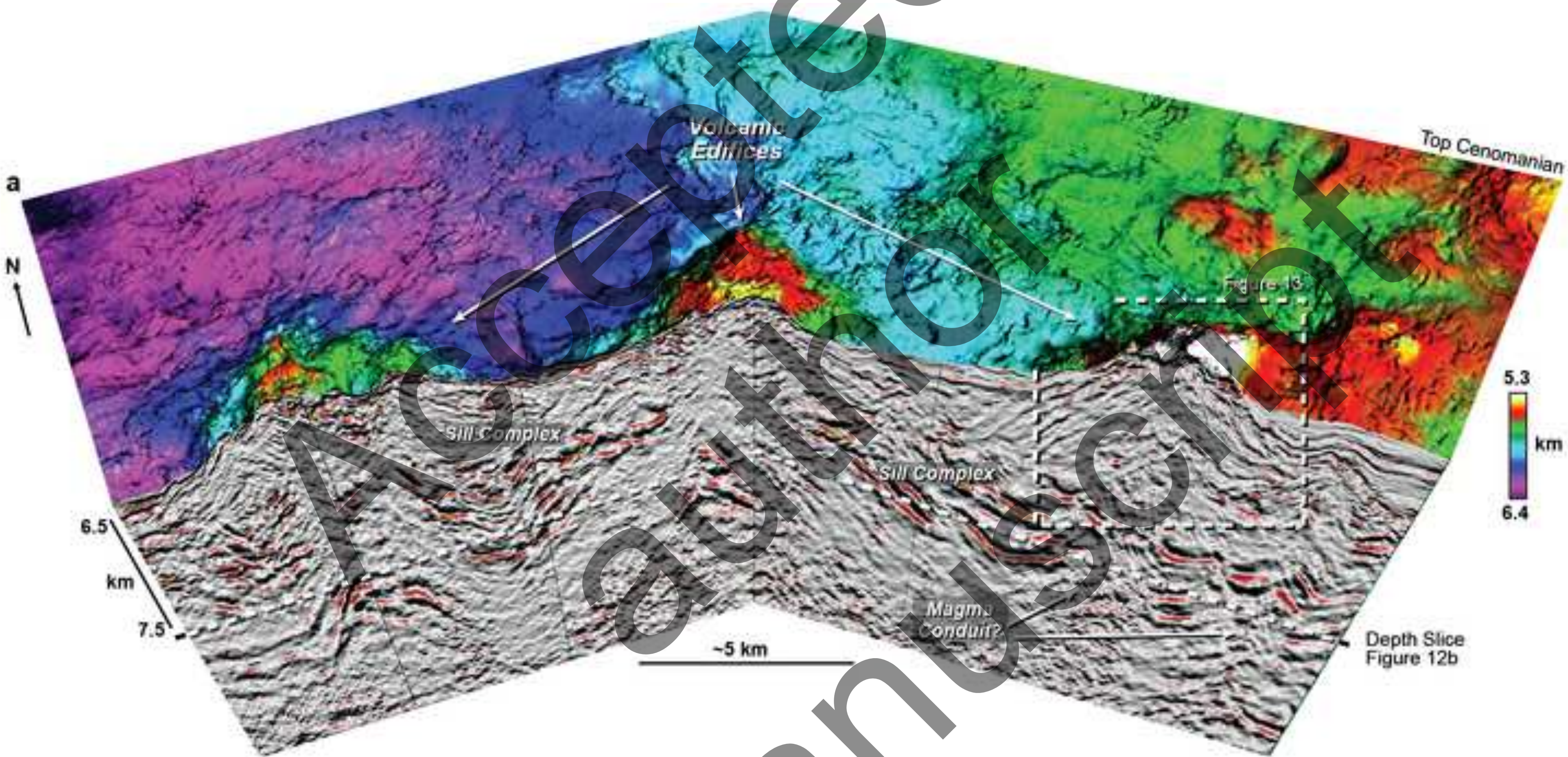
a
N
Volcanic Edifices
Top Cenomanian
Figure 13
Sill Complex
Sill Complex
Magma Conduit?
5.3
km
6.4
6.5
km
7.5
~5 km
Depth Slice Figure 12b

Figure12b

Click here to download Figure Figure12b.png

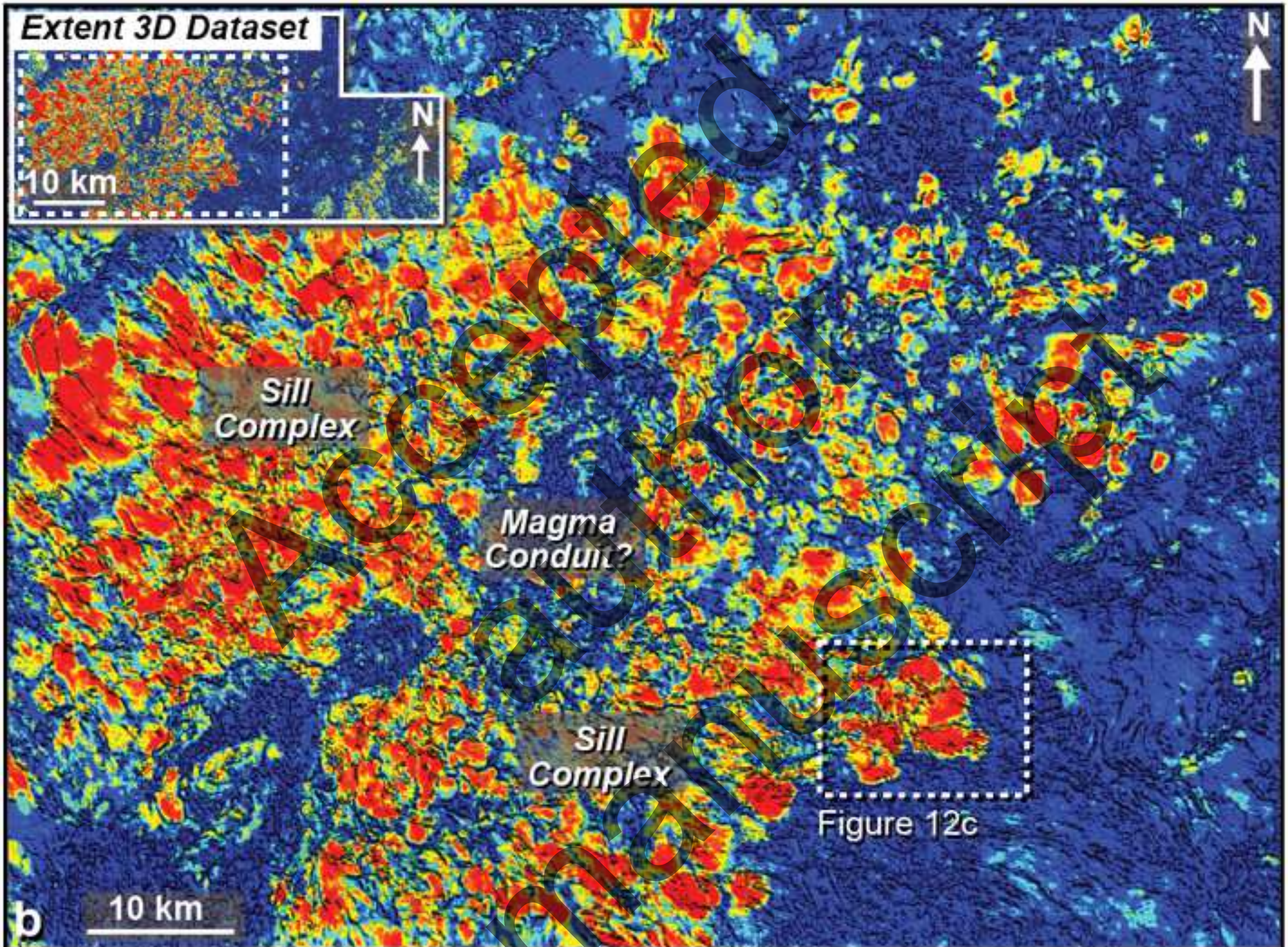

Figure12c

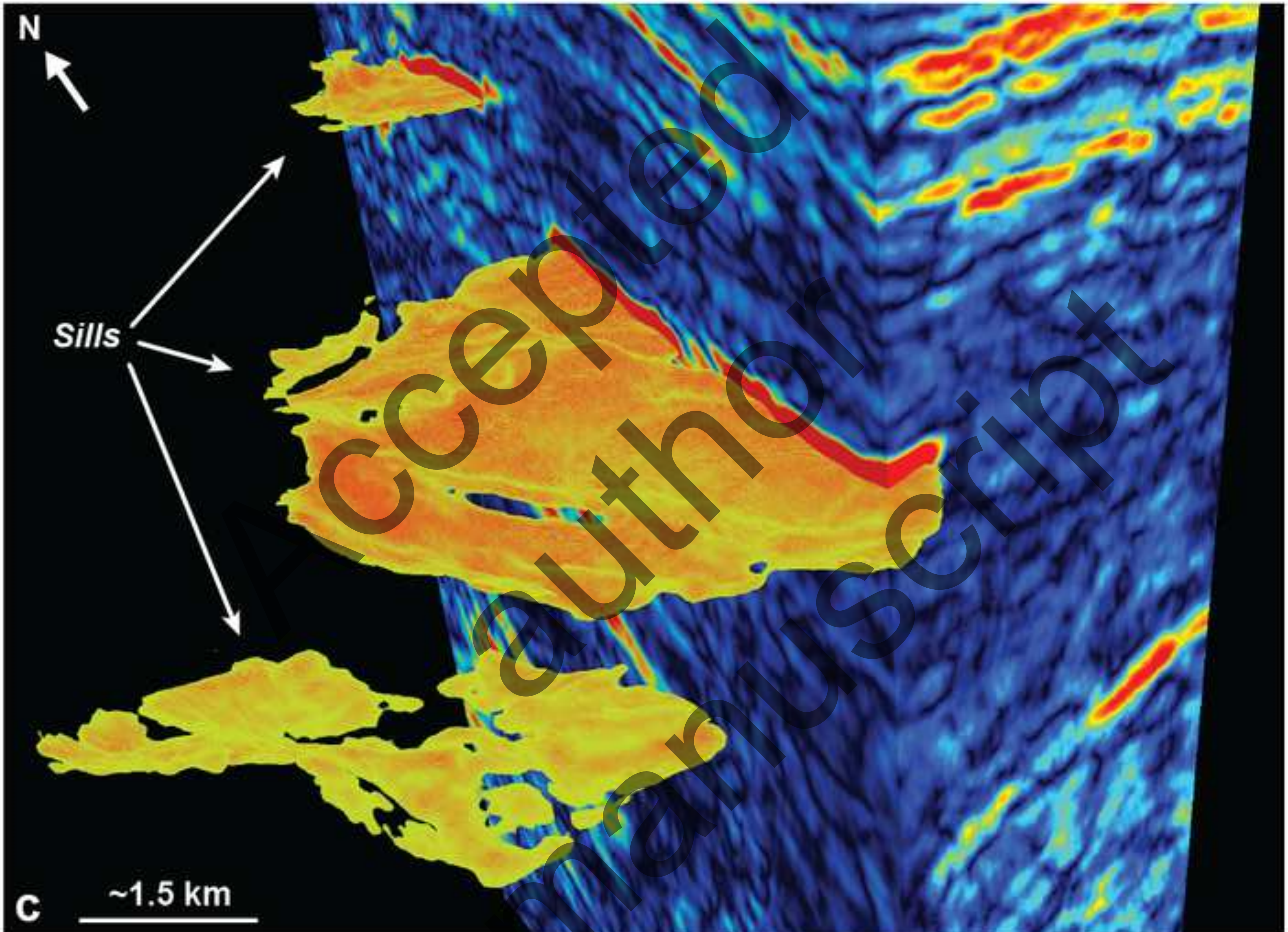

Figure13

Click here to download Figure Figure13.png

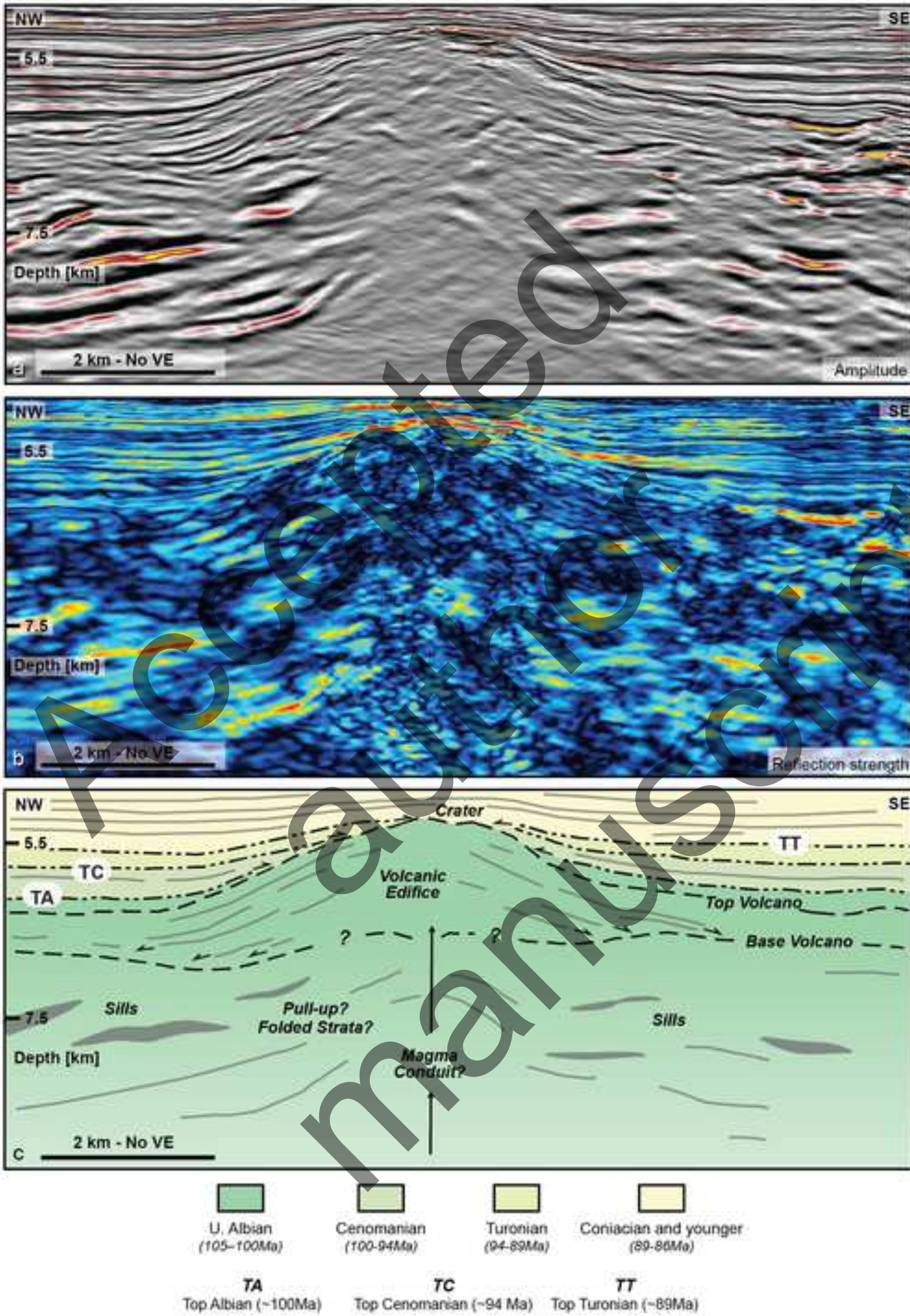

Figure14

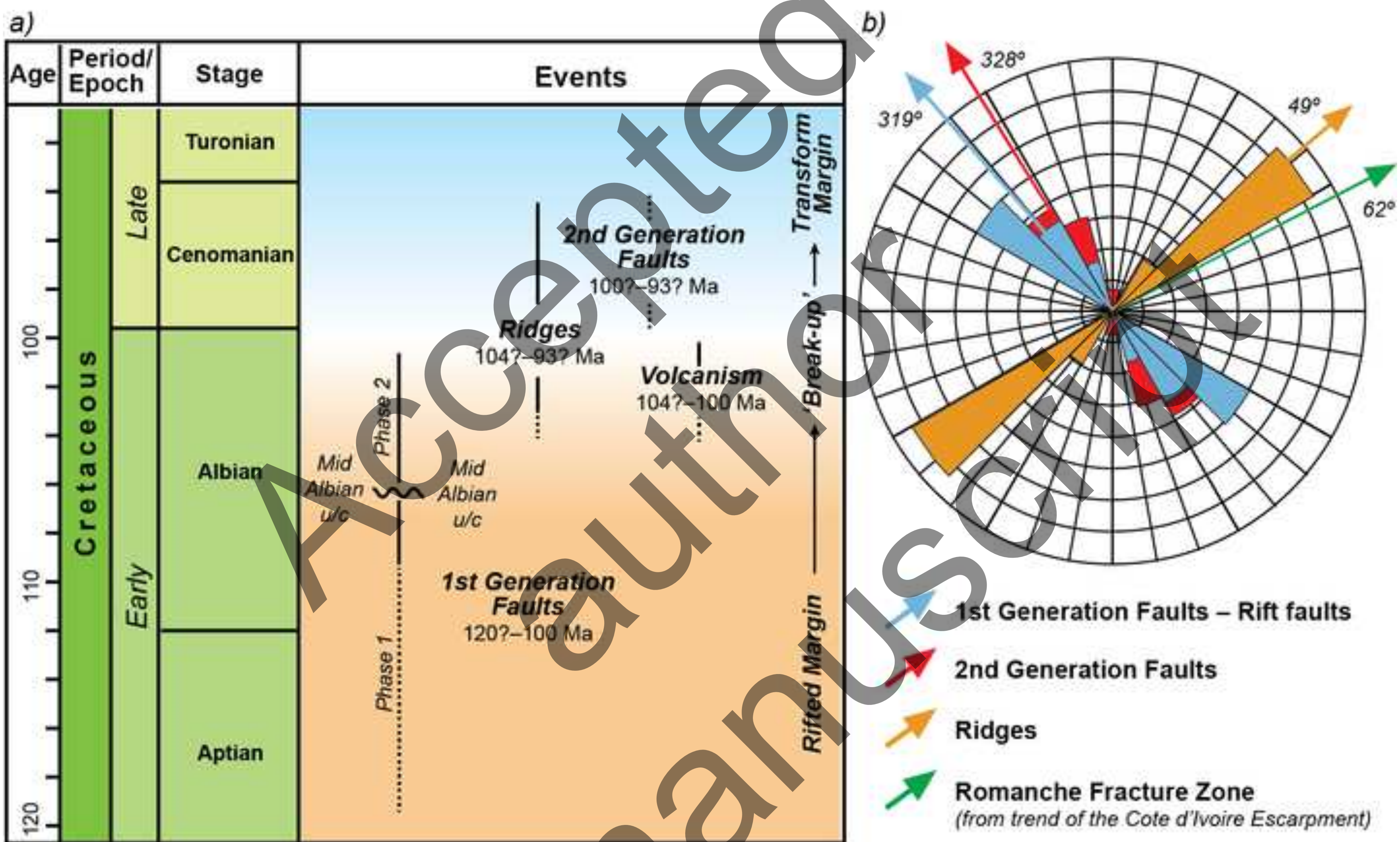

a)
Age
Period/ Epoch
Stage
Events
100
110
120
Cretaceous
Late
Early
Turonian
Cenomanian
Albian
Aptian
2nd Generation Faults
100?–93? Ma
Ridges
104?–93? Ma
Volcanism
104?–100 Ma
Mid Albian u/c
Mid Albian u/c
Phase 2
Phase 1
1st Generation Faults
120?–100 Ma
Transform Margin
'Break-up'
Rifted Margin
b)
328°
319°
49°
62°
1st Generation Faults – Rift faults
2nd Generation Faults
Ridges
Romanche Fracture Zone
(from trend of the Cote d'Ivoire Escarpment)

Figure15

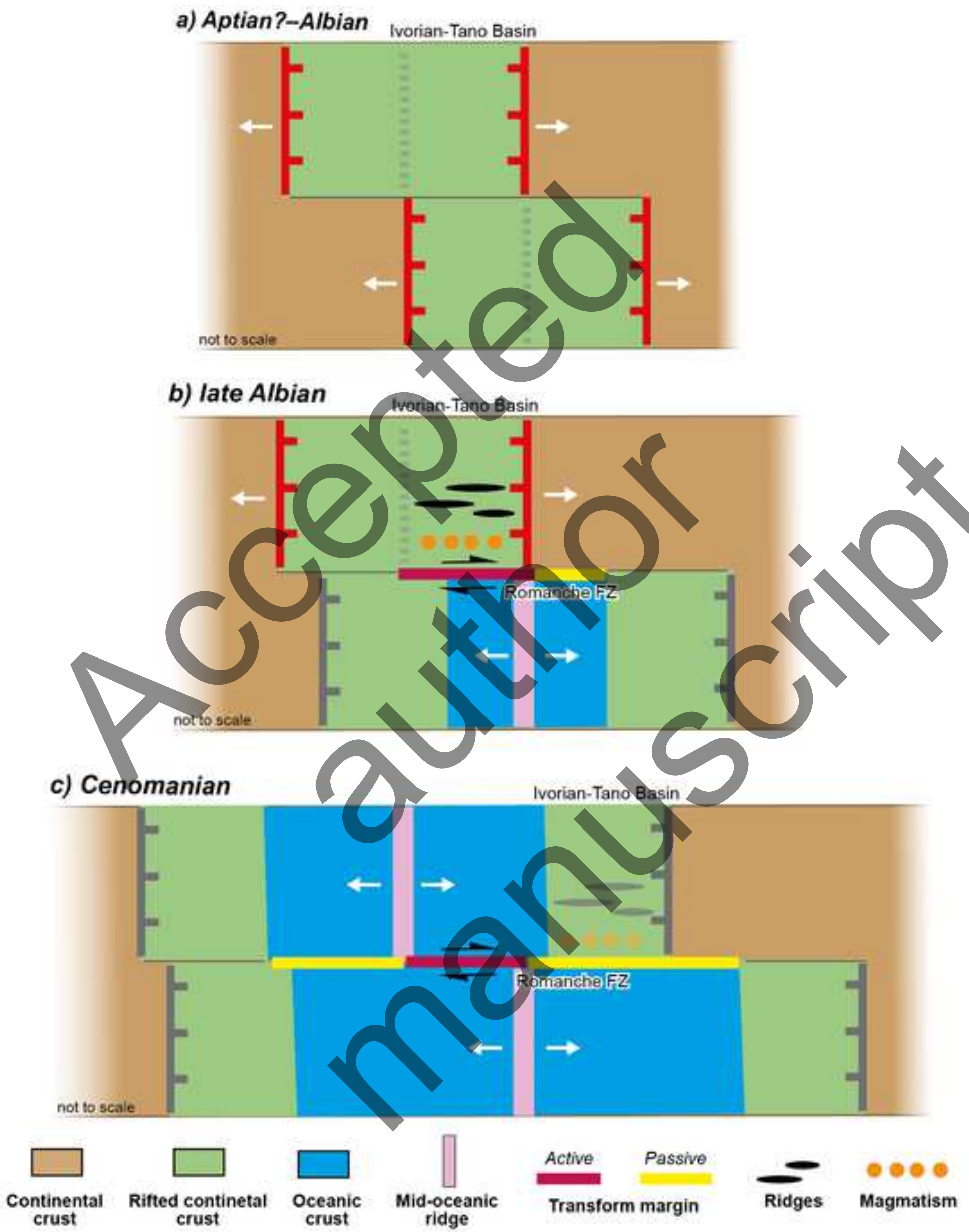
a) Aptian?–Albian
Ivorian-Tano Basin
not to scale
b) late Albian
Ivorian-Tano Basin
Romanche FZ
not to scale
c) Cenomanian
Ivorian-Tano Basin
Romanche FZ
not to scale
Continental crust
Rifted continetal crust
Oceanic crust
Mid-oceanic ridge
Active
Passive
Transform margin
Ridges
Magmatism